Commun. Math. Res. doi: 10.4208/cmr.2025-0002

Reduced Basis Method Based on Fourier Transform for Time-Dependent Parameterized Nonlocal Problems

Dou Dai¹, Huailing Song^{1,2} and Yuming Ba^{3,*}

- ¹ School of Mathematics, Hunan University, Changsha 410082, P.R. China.
- ² Greater Bay Area Institute for Innovation, Hunan University, Guangzhou 511340, P.R. China.

Received 11 January 2025; Accepted 13 March 2025

Abstract. In the paper, a reduced basis (RB) method for time-dependent nonlocal problems with a special parameterized fractional Laplace kernel function is proposed. Because of the lack of sparsity of discretized nonlocal systems compared to corresponding local partial differential equation (PDE) systems, model reduction for nonlocal systems becomes more critical. The method of snapshots and greedy (MOS-greedy) algorithm of RB method is developed for nonlocal problems with random inputs, which provides an efficient and reliable approximation of the solution. A major challenge lies in the excessive influence of the time domain on the model reduction process. To address this, the Fourier transform is applied to convert the original time-dependent parabolic equation into a frequency-dependent elliptic equation, where variable frequencies are independent. This enables parallel computation for approximating the solution in the frequency domain. Finally, the proposed MOS-greedy algorithm is applied to the nonlocal diffusion problems. Numerical results demonstrate that it provides an accurate approximation of the full order problems and significantly improves computational efficiency.

AMS subject classifications: 65N99, 60H35, 35R60

Key words: Nonlocal problems, reduced basis method, method of snapshots, greedy algorithm, Fourier transform.

³ School of Mathematics and Systems Science, Guangdong Polytechnic Normal University, Guangzhou 510065, P.R. China.

^{*}Corresponding author. *Email addresses:* ddou1008@hnu.edu.cn (D. Dai), shling@hnu.edu.cn (H. Song), yumingba@gpnu.edu.cn (Y. Ba)

1 Introduction

Historically, continuum models were predominantly described by partial differential equations (PDEs) based on local information. Later, the study of complex systems with singularities and anomalies, as well as those involving nonlocal interactions, became the focus. Nonlocal equations have been shown to provide significantly better models than their local counterparts in various applications. Examples include optimal control problems involving the Bellman equation derived from Levy processes, denoising models in nonlocal image processing [4,26], and particle systems modeling the nonlocal porous medium equation, the Hamilton-Jacobi equation with fractional diffusion [10,27], and conservation laws with fractional diffusion [7], among others.

Initial research on nonlocal models focused primarily on scalar problems [26, 30], with applications in image processing and steady-state diffusion, respectively. Subsequently, Du et al. established a more systematic mathematical framework for nonlocal problems parallel to classical local PDEs. They developed the nonlocal vector calculus [15, 16], and extensive research followed on functional analysis of nonlocal spaces, operators, and calculus of variations [21, 32, 41, 42]. Since exact solutions to nonlocal models are generally unavailable, numerical solutions posed new challenges for algorithm development and numerical analysis. This necessitated the development of robust and adaptive algorithms, as well as various numerical approximation schemes for nonlocal models [18-20]. Various applications of nonlocal models and connections to existing mathematical studies and numerical techniques have enabled nonlocal modeling to bridge the gap between multiscale modeling, analysis, and simulation [13,17,43]. Further rigorous mathematical analysis of nonlocal models was provided in [2,22]. In recent years, nonlocal models have been used in many areas, such as phase transition [2,23], nonlocal peridynamic models [1,40], nonlocal dispersal models [6,11] and option pricing in models with jumps [38].

Although nonlocal modeling can complement or replace traditional local modeling approaches based on PDEs, a priori for the value of the parameters in nonlocal kernel functions is unknown in practical scenarios involving modeling and prediction. In such case, an approximate solution is required not only as a function of a spatial variable but also as a function of model parameters. Compared to local models, the coefficient matrix of the discrete system for nonlocal models is typically dense, leading to higher computational costs. Therefore, reduced order models (ROMs) are necessary to approximate solutions efficiently, reducing computational costs. In this paper, the primary focus and challenge lie in selecting an appropriate model reduction method and accurately capturing the essential

features of the original system. For solving parameter-dependent PDE problems, we employ the reduced basis (RB) method, which is a very efficient numerical approximation method.

In practice, ROMs are widely used to replace the full order model with lower numerical complexity [8, 37, 39, 45]. For different problems, the strategies of constructing ROMs varied. The RB approach projects the full order model onto a subspace spanned by selected basis functions. These basis functions are derived from the singular value decomposition (SVD) of a set of full order solutions corresponding to chosen parameters. The first theoretical analysis of RB methods related to the continuation method for parametric equations was provided by Fink et al. [24,25]. Through the construction of basis functions, they systematically divided the calculation process into offline and online phases. For ROMs, posterior error estimates were employed to ensure the reliability of numerical solutions. However, in earlier methods, the approximate space tended to be fairly local due to the lack of a posterior error estimator and an efficient sampling procedure, and the parameters were often low-dimensional. Thus, significant efforts in the RB framework have focused on posterior error estimation procedures, particularly rigorous error bounds and efficient sampling strategies for outputs of interest in high-dimensional problems [12,44]. Error estimators play an important role in the sampling process of greedy algorithms [35,36], which are similar to the proper orthogonal decomposition (POD) method but methodologically distinct [3]. The POD does not select parameters. The greedy algorithm is typically applied to the multidimensional parameter domain, while the POD is most commonly applied to the one-dimensional temporal domain. The effective combination of these two techniques in parameter-time domains is often used to address parabolic problems [33, 35].

In recent work on model reduction methods for nonlocal problems, Guan *et al.* developed RB approximations for nonlocal diffusion equations with affine random coefficients and established efficiency estimates of the proposed greedy algorithms [28]. Burkovska *et al.* developed the RB method for parameterized problems driven by spatially nonlocal integral operators with parameter-dependent kernels. For problems with nonaffine, singular, or discontinuous kernels, the regularity and differentiability results with respect to parameters were derived and then used to construct affine approximations of the kernels by local polynomials [29]. However, these methods were primarily applied to model reduction for steady-state nonlocal equations with random inputs. For dynamic nonlocal diffusion equations, D'Elia *et al.* developed a model reduction framework [47], where the parameters were derived from the equation coefficients. This differs from our approach, where the parameters are derived from the kernel function.

In this work, we focus on developing the RB approximations for parameterized time-dependent nonlocal problems. The form of nonlocal kernel functions with random parameters is detailed in Section 2. Before the reduction, we employ the Fourier transform to convert the original time-dependent parabolic equation into a frequency-dependent elliptic equation [31]. Without this transformation, the full order model after numerical discretization was directly used for the model reduction. The results contradicted our expectations. We observed that the temporal term significantly influenced the model reduction. When using the Fourier transform, the influence of time is avoided, and the original recursive relationship is converted into parallel algorithms. This enhances computational efficiency. We employ the method of snapshots (MOS) [46] to construct lower-dimensional basis functions by computing the eigenvectors of the snapshot covariance matrix. The RB method then projects the solution space onto a lowdimensional subspace spanned by the basis functions. The efficiency of the RB method is enhanced through offline-online computational decomposition. In the offline phase, snapshots and basis functions are computed. In the online phase, solutions are repeatedly computed for random parameters using ROMs. To obtain snapshots, traditional numerical methods such as the finite volume method (FVM), finite difference method (FDM), finite element method (FEM), and their variations can be employed to solve full order models. Furthermore, the integration kernel in this paper is nonaffine, singular, and discontinuous. For nonaffine parameter dependencies and nonlinear terms, we adopt the Chebyshev interpolation [29] and the discrete empirical interpolation method (DEIM) [9]. To the end, we apply the Fourier transform to the time-dependent nonlocal model and develop a nonlocal model reduction method by integrating the nonlocal frequency equation into the RB framework.

The rest of the paper is organized as follows. In Section 2, we introduce the parameterized time-dependent nonlocal problems and variational formulations. The specific reduction procedure and posterior error estimates are shown in Section 3. In Section 4, the MOS-greedy algorithm for the parameterized time-dependent nonlocal problems is proposed to construct the basis functions. Numerical examples with linear and nonlinear terms are presented in Section 5. Finally, Section 6 gives some conclusions and comments.

2 Preliminaries and notations

In this section, we introduce the notion of nonlocal problems and propose a concept of frequency transformations when they are applied to time-dependent non-

local problems. Moreover, this section covers the numerical approximation methods for frequency transformation and inverse transformation, as well as specific forms for handling nonaffine parameters.

2.1 Nonlocal diffusion model

In this paper, we propose and analyze the following parameterized nonlocal and nonlinear diffusion equation with the volume-constrained:

$$\begin{cases}
\frac{\partial u(x,t,s)}{\partial t} = \frac{2(1-s)}{\delta^{2-2s}} \mathcal{L}_{\delta} u(x,t,s) \\
+f(x,t,s) + h(u(x,t,s),t,s), & x \in \Omega, \quad t \in [0,T], \\
u(x,t,s) = g(x,t,s), & x \in \Gamma, \quad t \in [0,T], \\
u(x,0,s) = u_0, & x \in \overline{\Omega}.
\end{cases} \tag{2.1}$$

Here $\Omega=(a,b)\subset\mathbb{R}$ is the bounded domain, $\overline{\Omega}$ denotes the closure of Ω , $x\in R$ is the spatial variable, $t\in[0,T]$ is the temporal variable with T>0 as the final computation time, and $s\in\mathcal{P}^s\subset(0,1)$ is the parametric variable. The terms f and h represent the linear and nonlinear components, respectively, while g is the boundary condition and u_0 is the initial condition. The set $\Gamma=\overline{\Omega'}\setminus\Omega=[a-\delta,a]\cup[b,b+\delta]$ is illustrated in Fig. 1. The operator \mathcal{L}_δ is nonlocal, and the parameter $\delta>0$ represents the range of nonlocal interaction. To account for nonlocal spatial interactions, nonlocal operators usually use integral forms to avoid explicitly using spatial derivatives. The nonlocal operator is specifically expressed as follows:

$$-\mathcal{L}_{\delta}u(x,t,s) = 2\int_{\Omega} \left(u(x,t,s) - u(x',t,s) \right) \gamma(x,x';s) dx', \tag{2.2}$$

where $\gamma(x,x';s)$ is a nonnegative symmetric kernel function. There is a detailed description of such kernel functions in [15, 29], where the well-posedness of all these kernels for nonlocal problems has been demonstrated.

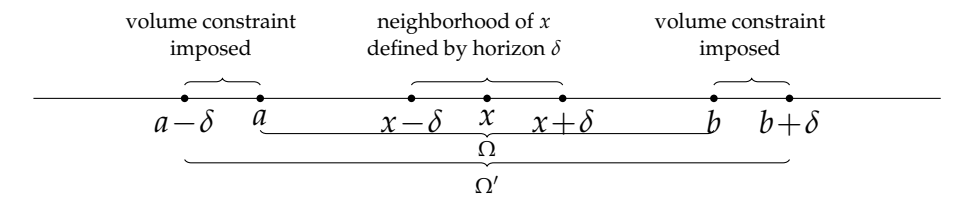


Figure 1: The domain of definitions for nonlocal problems.

There are two main types of kernel functions, one is called a general truncated kernel function, for $\delta > 0$, we define a ball $B_{\delta}(x)$ centered at x with radius δ , i.e., $B_{\delta}(x) := \{x' \in \mathbb{R} : |x - x'| \le \delta\}$. Then for $0 < \delta_{\min} < \delta_{\max} < \infty$ and all $x \in \mathbb{R}$ satisfy

$$\begin{cases}
\gamma(x,x';\delta) \ge 0, & \forall x' \in B_{\delta}(x), \\
\gamma(x,x';\delta) = 0, & \forall x' \in \mathbb{R} \setminus B_{\delta}(x), \\
\gamma(x,x';\delta) \ge \gamma_0 > 0, & \forall x' \in B_{\delta_{\min/2}}(x),
\end{cases}$$
(2.3)

where γ_0 is a nonnegative constant. The other is a special focus in this paper and will lie on fractional Laplace-type kernels, where the kernel parameter is a fractional power $s \in (0,1)$ and defined as follows:

$$\gamma(x,x';s) = \begin{cases} \frac{1}{|x-x'|^{1+2s}}, & x' \in B_{\delta}(x), \\ 0, & \text{otherwise.} \end{cases}$$
 (2.4)

Here δ is a given parameter. When $\delta \to +\infty$, (2.4) is a classical fractional Laplace kernel and $-\mathcal{L}_{\delta}$ reduces to the fractional Laplace operator $(-\Delta)^s$ up to the constant $c_s/2$ where

$$c_s = \frac{2^{2s} s \Gamma(s+1/2)}{\pi^{1/2} \Gamma(1-s)},\tag{2.5}$$

see [15] for more details. When $\delta \to 0$, the nonlocal operator $-(2(1-s)/\delta^{2-2s})\mathcal{L}_{\delta}$ reduces to the local Laplace operator $-\Delta$. The local limit form of the nonlocal problem (2.1) is given by

$$\begin{cases}
\frac{\partial u(x,t,s)}{\partial t} = -\Delta u(x,t,s) \\
+f(x,t,s) + h(u(x,t,s),t,s), & x \in \Omega, & t \in [0,T], \\
u(x,t,s) = g(x,t,s), & x \in \partial \Omega, & t \in [0,T], \\
u(x,0,s) = u_0, & x \in \overline{\Omega}.
\end{cases}$$
(2.6)

In [14], the convergence of approximate nonlocal solutions to the solution of the Laplace equation is established. By comparing Eqs. (2.1) and (2.6), we observe that linear integral operators are used in nonlocal models, in contrast to the linear differential operators employed in local diffusion models. Additionally, the Dirichlet condition imposed on the boundary in local models becomes a volume constraint in nonlocal problems.

2.2 The frequency space of nonlocal problems

Traditionally, (2.1) is solved in space-time by time discretization such as Crank-Nicholson or Runge-Kutta method. Although these methods can effectively solve a wide range of practical problems, they rely on recursive temporal relationships and lack natural parallelizability. To reduce computation costs, we apply the frequency domain method to solve time-dependent nonlocal problems. This approach enables efficient parallel computation due to the mutual independence of frequencies. One of the frequency domain methods is the Fourier transform. The Fourier transform and Fourier inversion of a function $u(\cdot,t)$ in time are given by

$$\hat{u}(\cdot,\omega) = \int_{-\infty}^{\infty} u(\cdot,t) \exp(-i\omega t) dt,$$

$$u(\cdot,t) = \frac{1}{2\pi} \int_{-\infty}^{\infty} \hat{u}(\cdot,\omega) \exp(i\omega t) d\omega.$$

The Fourier transformation is used for time and then converts the original problem (2.1) into a set of complex elliptic equations that depend on the frequency ω , i.e.,

$$i\omega\hat{u}(x,\omega,s) = \frac{2(1-s)}{\delta^{2-2s}} \mathcal{L}_{\delta}\hat{u}(x,\omega,s) + \hat{f}(x,\omega,s) + \hat{h}(\hat{u},\omega,s), \tag{2.7a}$$

$$\hat{u}(x,\omega,s) = \hat{g}(x,\omega,s), \quad x \in \Gamma, \tag{2.7b}$$

where f,h and u are extended to be zero when t < 0 and t > T for the Fourier transformation. Let $\Omega \subset \mathbb{R}$ be an open set for $s \in (0,1)$. The real-valued fractional Sobolev space $H^s(\Omega)$ is defined as

$$H^{s}(\Omega) := \left\{ u \in L^{2}(\Omega) : |u|_{H^{s}(\Omega)}^{2} = \int_{\Omega} \int_{\Omega} \frac{|u(x) - u(x')|^{2}}{|x - x'|^{1 + 2s}} dx' dx < \infty \right\}.$$

Equipped with the norm

$$\|\cdot\|_{H^s(\Omega)} = \|\cdot\|_{L^2(\Omega)} + |\cdot|_{H^s(\Omega)},$$

 $H^s(\Omega)$ forms a Hilbert space. In this paper, assume that an arbitrary complex value function $\hat{u} = \hat{u}_r + i\hat{u}_i$, where \hat{u}_r and \hat{u}_i represent the real and imaginary parts, respectively. The inner product and norm in the complex space are defined as

$$(\hat{u},\hat{v})_c := \int_{\Omega} \hat{u}\bar{v}dx = (\hat{u},\bar{v})_{L^2}, \quad \|\hat{u}\|_c := (\|\hat{u}_r\|_{L^2}^2 + \|\hat{u}_i\|_{L^2}^2)^{\frac{1}{2}}.$$

Let

$$H_c^s(\Omega) := H^s(\Omega) \times H^s(\Omega), \quad L_c^2(\Omega) := L^2(\Omega) \times L^2(\Omega),$$

we define the space incorporating the volume constraints, given by

$$H_{\Omega}^s := \{ \hat{u} \in H_c^s(\Omega) : \hat{u} = \hat{g} \text{ on } \Gamma \}.$$

The bilinear form is defined as

$$a(\hat{u},\hat{v};s)_{c} := \iint_{\Omega \times \Omega} \left(\hat{u}(x,\omega,s) - \hat{u}(x',\omega,s) \right) \left(\overline{\hat{v}(x) - \hat{v}(x')} \right) \gamma(x,x';s) d(x',x). \tag{2.8}$$

We define the spaces

$$X := \left\{ \hat{u} \in L^2(\Omega \cup \Gamma) : a(\hat{u}, \hat{u}; s)_c < +\infty \right\},$$

$$V := \left\{ \hat{u} \in X : \hat{u} = \hat{g} \text{ on } \Gamma \right\}$$

as a nonlocal frequency domain space and a constrained nonlocal frequency domain space with a fractional Laplace kernel, respectively. The inner product and norm on V are defined as

$$(\hat{u},\hat{v})_V := a(\hat{u},\hat{v};s)_c, \quad \|\hat{u}\|_V^2 = (\hat{u},\hat{u})_V.$$

The fractional Laplace kernel satisfies the nonlocal Poincaré inequality [15]

$$\|\hat{u}\|_{L^2(\Omega \cup \Gamma)} \le C_p \|\hat{u}\|_V, \quad \forall \hat{u} \in V, \tag{2.9}$$

where $C_p > 0$ is the Poincaré constant.

From the nonlocal spatial definition and the nonlocal Poincaré inequality, the nonlocal space V is equivalent to H_{Ω}^s , which implies

$$C\|\hat{u}\|_{H_{\Omega}^{s}} \le \|\hat{u}\|_{V} \le \|\hat{u}\|_{H_{\Omega}^{s}}.$$
 (2.10)

By this equivalence, the bilinear form $a(\cdot,\cdot;s)_c$ defined in (2.8) is continuous and coercive in $V \times V$, that is, for $\forall \hat{u}, \hat{v} \in V$, $\exists \beta_0 > 0$ such that

$$\alpha(s) := \sup_{\hat{u} \in V} \sup_{\hat{v} \in V} \frac{a(\hat{u}, \hat{v}; s)_c}{\|\hat{u}\|_V \|\hat{v}\|_V} < +\infty, \quad \forall s \in (0, 1),$$
(2.11)

$$\beta(s) := \inf_{\hat{u} \in V} \frac{a(\hat{u}, \hat{u}; s)_c}{\|\hat{u}\|_V^2} \ge \beta_0, \qquad \forall s \in (0, 1).$$
 (2.12)

2.3 Variational formulation for the nonlocal problems

The finite element discretization of the nonlocal frequency domain model (2.7) is based on the weak form of the problem. In this section, we present the weak form of the nonlocal equation. The variational formulation can be defined in a way similar to the local model, except that the volume constraint replaces the boundary condition. This ensures the regularity of the nonlocal Dirichlet problem.

Multiplying Eq. (2.7a) by the test function $\hat{v}(x) \in V$ for $\forall \omega \in \mathbb{R}$, then the integral form in the bounded domain Ω is given by

$$\int_{\Omega} i\omega \hat{u}(x,\omega,s)\bar{\hat{v}}(x)dx + \frac{4(1-s)}{\delta^{2-2s}} \int_{\Omega} \bar{\hat{v}}(x)dx
\times \int_{B_{\delta}(x)} (\hat{u}(x,\omega,s) - \hat{u}(x',\omega,s)) \gamma(x,x';s)dx' - \int_{\Omega} \hat{h}(\hat{u},\omega,s)\bar{\hat{v}}(x)dx
= \int_{\Omega} \hat{f}(x,\omega,s)\bar{\hat{v}}(x)dx.$$
(2.13)

Note that the double integral term in (2.13) leads to an asymmetric finite element stiffness matrix. To avoid the asymmetric matrix, Eq. (2.13) by using the nonlocal Green's first identity derived in [16] (or by direct calculation) is equivalent to

$$\int_{\Omega} i\omega \hat{u}(x,\omega,s)\bar{v}(x)dx + \frac{2(1-s)}{\delta^{2-2s}} \times \int_{\Omega} \int_{B_{\delta}(x)} \left(\hat{u}(x,\omega,s) - \hat{u}(x',\omega,s)\right) \left(\bar{v}(x) - \bar{v}(x')\right) \gamma(x,x';s)dx'dx \\
- \int_{\Omega} \hat{h}(\hat{u},\omega,s)\bar{v}(x)dx \\
= \int_{\Omega} \hat{f}(x,\omega,s)\bar{v}(x)dx. \tag{2.14}$$

Therefore, the weak form of this nonlocal problem is as shown in Eq. (2.15). For a given $\hat{g}(x,\omega,s)$ and $\forall \omega \in \mathbb{R}$, there exists a $\hat{u}(x,\omega,s) \in V$ such that

$$i\omega(\hat{u},\hat{v})_c + \frac{2(1-s)}{\delta^{2-2s}}a(\hat{u},\hat{v};s)_c - (\hat{h},\hat{v})_c = (\hat{f},\hat{v})_c, \quad \forall \hat{v} \in V,$$
 (2.15a)

$$\hat{u}(x,\omega,s) = \hat{g}(x,\omega,s), \qquad x \in \Gamma.$$
 (2.15b)

Let $V^{\mathcal{N}} \subset V$ be the FE approximation space, where \mathcal{N} is sufficiently large. Assume $V^{\mathcal{N}} = P_h \bigoplus i P_h$, where P_h is the standard piecewise linear real-valued finite element

subspace of H^s_{Ω} with $\dim(P_h) = \mathcal{N}$. Let $\{\phi_j\}_{j=1}^{\mathcal{N}}$ be a set of the nodal basis of P_h . For a given $s \in (0,1)$, there exists $\hat{u}^{\mathcal{N}}(\omega,s) = \hat{u}^{\mathcal{N}}(x,\omega,s) \in V^{\mathcal{N}}$ satisfying

$$i\omega(\hat{u}^{\mathcal{N}}(\omega,s),\hat{v})_{c} + \frac{2(1-s)}{\delta^{2-2s}}a(\hat{u}^{\mathcal{N}}(\omega,s),\hat{v};s)_{c} - (\hat{h}(\hat{u}^{\mathcal{N}}(\omega,s)),\hat{v})_{c} = (\hat{f},\hat{v})_{c}, \quad \forall \hat{v} \in V^{\mathcal{N}}.$$

$$(2.16)$$

For $\forall \omega \in \mathbb{R}$, $\hat{u}^{\mathcal{N}}(\omega,s) \in V^{\mathcal{N}} = P_h \bigoplus iP_h$ can be expressed as

$$\hat{u}^{\mathcal{N}}(\omega,s) = \sum_{j=1}^{\mathcal{N}} u_j^R(\omega,s)\phi_j + i\sum_{j=1}^{\mathcal{N}} u_j^I(\omega,s)\phi_j. \tag{2.17}$$

Combining Eqs. (2.16) and (2.17), we have the following nonlinear system of order $2\mathcal{N}$:

$$\begin{bmatrix} \mathbf{M}^{\omega} + \mathbf{A} & -\mathbf{M}^{\omega} + \mathbf{A} \\ \mathbf{M}^{\omega} - \mathbf{A} & \mathbf{M}^{\omega} + \mathbf{A} \end{bmatrix} \begin{bmatrix} \mathbf{u}^{R}(\omega, s) \\ \mathbf{u}^{I}(\omega, s) \end{bmatrix} - \begin{bmatrix} \mathbf{M} & \mathbf{M} \\ -\mathbf{M} & \mathbf{M} \end{bmatrix} \begin{bmatrix} \mathbf{h}^{R} \\ \mathbf{h}^{I} \end{bmatrix} = \begin{bmatrix} \mathbf{f}^{R} + \mathbf{f}^{I} \\ -\mathbf{f}^{R} + \mathbf{f}^{I} \end{bmatrix}, \quad (2.18)$$

where

$$M^{\omega}(p,q) = \omega(\phi_p,\phi_q)_c, \quad A(p,q) = \frac{2(1-s)}{\delta^{2-2s}} a(\phi_p,\phi_q;s)_c,
M(p,q) = (\phi_p,\phi_q)_c, \quad p,q = 1,...,\mathcal{N},$$

and $\boldsymbol{h}^R, \boldsymbol{h}^I, \boldsymbol{f}^R, \boldsymbol{f}^I \in \mathbb{R}^{\mathcal{N}}$ are given by

$$\mathbf{h}^{R} = \Re(\hat{h}(\mathbf{u}(\omega,s)), \quad \mathbf{h}^{I} = \Im(\hat{h}(\mathbf{u}(\omega,s)), \\
\mathbf{f}^{R}(q) = (\hat{f}^{R}, \phi_{q})_{c}, \quad \mathbf{f}^{I}(q) = (\hat{f}^{I}, \phi_{q})_{c}, \quad q = 1, \dots, \mathcal{N},$$

where

$$\begin{split} & \boldsymbol{u}(\omega,s) = \left\{ \hat{u}_q^{\mathcal{N}}(\omega,s) \right\}_{q=1}^{\mathcal{N}}, \quad \hat{f} = \hat{f}^R + i\hat{f}^I, \\ & \boldsymbol{u}^R(\omega,s) = \left\{ u_q^R(\omega,s) \right\}_{q=1}^{\mathcal{N}}, \quad \boldsymbol{u}^I(\omega,s) = \left\{ u_q^I(\omega,s) \right\}_{q=1}^{\mathcal{N}}. \end{split}$$

To convert frequency variables into time variables, the inverse Fourier transform will be used. For the inverse Fourier transform, we adopt the truncated integral interval $[0, \omega^*]$ with a sufficiently large $\omega^* > 0$ and use the nodes and weights of the Legendre-Gauss-Lobatto (LGL) integration rule to obtain $\hat{u}(\omega) =$

 $\hat{u}(x,\omega,s)$ [31]. Then the time domain real-valued solution u(x,t,s) of (2.1) is then approximated as

$$u(x,t,s) = \frac{1}{\pi} \Re \left(\sum_{j=1}^{N_{\omega}} \hat{u}^{\mathcal{N}}(x,\omega_j,s) \exp(i\omega_j t) \mathbf{w}_j \right), \tag{2.19}$$

where ω_j and w_j are the LGL interpolation nodes and corresponding weights on the interval $[0, \omega^*]$, respectively.

2.4 Affine approximation

In this paper, we consider the fractional Laplace kernel defined in Eq. (2.4). The dependence on the parameter s is nonaffine in this case, the nature of the singularity changes with the parameter. This leads to the different regularity of the solution. Furthermore, the integration kernel is discontinuous at $|x-x'|=\delta$ and has a singularity at $|x-x'|\to 0$. This prevents the direct application of empirical interpolation, as it is designed for continuous and bounded functions. Although the continuity requirement can be relaxed using a generalized empirical interpolation method, selecting an appropriate interpolating functional in the current context is non-trivial. To obtain the affine form of the parameters for the kernel function, we employ local polynomials to approximate the nonaffine form [29], i.e., splitting the interval $\mathcal{P}^s := [s_{\min}, s_{\max}] \subset [0,1]$,

$$0 < s_{\min} := s_0 < s_1 < \dots < s_M =: s_{\max} < \infty, M \in \mathbb{N}.$$

Then for a given $\delta \in (0,\infty)$, $s \in (0,1)$, and sufficiently regular \hat{u}, \hat{v} , there is

$$a(\hat{u},\hat{v};s)_{c} \approx \widetilde{a}_{M}(\hat{u},\hat{v};s)_{c} := \sum_{m=0}^{M} \Theta_{m}^{s}(s) a(\hat{u},\hat{v};s_{m})_{c}, \quad \Theta_{m}^{s}(s) := \prod_{\substack{j=0 \ j \neq m}} \frac{s-s_{j}}{s_{m}-s_{j}}, \quad (2.20)$$

where s_m is the maximum value of Chebyshev in the interval $[s_{\min}, s_{\max}]$, that is,

$$s_m = \frac{1}{2(s_{\min} + s_{\max})} - \frac{1}{2(s_{\max} - s_{\min})} \cos\left(\frac{m}{M}\pi\right), \quad m = 0, ..., M.$$

In practice, the coefficients Θ_m^s may be negative. This leads to the coercive condition of $\tilde{a}_M(\cdot,\cdot;\cdot)_c$ on $V\times V$ is failed. To address this issue, we introduce

$$\tilde{a}_{M,\rho}(\hat{u},\hat{v};s)_c = \tilde{a}_M(\hat{u},\hat{v};s)_c + \rho a(\hat{u},\hat{v};\hat{s})_c$$
 (2.21)

with a regularization parameter $\rho > 0$, where

$$\hat{s} = \frac{s_1 + s_2}{2} = \begin{cases} s_{\min} + \frac{1}{4} - \frac{\varepsilon}{2}, & \text{if } s_{\min} \le \frac{1}{2}, \\ \frac{s_{\min} + 1}{2} - \frac{\varepsilon}{2}, & \text{otherwise} \end{cases}$$

for arbitrarily small $\varepsilon > 0$.

Remark 2.1. In fact, the regularization parameter $\rho > C(\delta)\sigma^{M+1}$, where $C(\delta)$ is a constant depending on δ . This parameter ensures coercivity. When $\sigma < 1$, this term is numerically negligible. In order to ensure $\sigma < 1$, we require that

$$s_1 = s_{\min}$$
, $s_2 = s_{\min} + \frac{1}{2} - \varepsilon$, for $s_{\min} \le \frac{1}{2}$ and $s_{\max} - s_{\min} < \frac{1}{5}$, $s_1 = s_{\min}$, $s_2 = 1 - \varepsilon$, for $s_{\min} > \frac{1}{2}$ and $s_{\max} - s_{\min} < \frac{2}{3(1 - s_{\max})}$.

In the practical application, it is not possible that every interval can meet exactly the above requirements. To address this, we can divide the large intervals $[s_{\min}, s_{\max}]$ into several subintervals $[s_{\min}^j, s_{\max}^j]$, each of which is connected end-to-end, that is, $s_{\max}^{j-1} = s_{\min}^j$, so that as long as the subintervals meet the above requirements.

3 Reduced basis methods

ROMs have been widely used to reduce the computational cost of approximating solutions to local PDEs. However, the model reduction of nonlocal models is limited, such as the models considered in this paper. The nonlocal model equations are parameterized time-dependent problems. In this paper, the nonlocal PDEs are spatially discretized using the FEM. Furthermore, the methods discussed below are also applicable to other discretization methods.

The underlying discrete system is composed of a band matrix with a bandwidth and a nonlocal interaction radius. Thus, solving the problems (2.1) with random input parameters by FEM requires expensive computation. In order to reduce the computational cost, we construct a ROM. In this section, we describe the construction of the RB approximation for (2.16). Given a positive integer N_{max} , we replace $V^{\mathcal{N}}$ with a low-dimensional RB approximation space $V^{\mathcal{N}}_N \subset V^{\mathcal{N}}$, where $N=1,2,\ldots,N_{\text{max}}$. These spaces are assumed to be nested (or hierarchical), i.e.,

 $V_1^{\mathcal{N}} \subset V_2^{\mathcal{N}} \subset \cdots \subset V_{N_{\max}}^{\mathcal{N}} \subset V^{\mathcal{N}}$.

The idea of the RB method is to construct the approximate solution of problem (2.16) in the low-dimensional subspace $V_N^{\mathcal{N}}(N \ll \mathcal{N})$. A sufficiently small N ensures low computational cost. However, several important conditions must be satisfied when using RB methods. First, the affine-parameter dependency of the problem is necessary to perform effective parameter-dependent operations in the online phase. Second, the separation of parameters and variables needs to be realized by using proper methods for the nonlinear terms. This can improve the online calculation. Finally, a computable posterior error estimate is necessary to enable an effective and accurate selection of input parameters in the offline phase.

3.1 Galerkin projection and offline-online procedure

We now consider the ROM. The RB approximation is defined as the Galerkin projection onto these low-dimensional subspaces, i.e., for any given $s \in \mathcal{P}^s$, $u_N(\omega, s) \in V_N^N$ satisfies

$$i\omega \left(u_N(\omega,s),v\right)_c + \frac{2(1-s)}{\delta^{2-2s}} \tilde{a}_{M,\rho} \left(u_N(\omega,s),v;s\right)_c - \left(\hat{h}\left(u_N(\omega,s),\omega,s\right),v\right)_c = (\hat{f},v)_c. \tag{3.1}$$

Let $\{\zeta_p^R\}_{p=1}^N$ and $\{\zeta_p^I\}_{p=1}^N$ denote the real and imaginary basis functions of V_N^N , respectively. Then the solutions $u_N(\omega,s)$ can be represented as

$$u_{N}(\omega,s) = \sum_{p=1}^{N} \zeta_{p}^{R} u_{N}^{R}(\omega,s) + i \sum_{p=1}^{N} \zeta_{p}^{I} u_{N}^{I}(\omega,s).$$
 (3.2)

Choosing the test functions $v = \zeta_q^R + i\zeta_q^I$, $1 \le q \le N$ and combining with (3.2), Eq. (3.1) can be represented as

$$\begin{split} &i\omega\sum_{p=1}^{N}\left(\zeta_{p}^{R},\zeta_{q}^{R}\right)_{c}u_{N}^{R}(\omega,s)+\omega\sum_{p=1}^{N}\left(\zeta_{p}^{R},\zeta_{q}^{I}\right)_{c}u_{N}^{R}(\omega,s)\\ &-\omega\sum_{p=1}^{N}\left(\zeta_{p}^{I},\zeta_{q}^{R}\right)_{c}u_{N}^{I}(\omega,s)+i\omega\sum_{p=1}^{N}\left(\zeta_{p}^{I},\zeta_{q}^{I}\right)_{c}u_{N}^{I}(\omega,s)\\ &+\sum_{p=1}^{N}\sum_{m=0}^{M}\Theta_{m}^{s}(s)\frac{2(1-s)}{\delta^{2-2s}}a\left(\zeta_{p}^{R},\zeta_{q}^{R};s_{m}\right)_{c}u_{N}^{R}(\omega,s)\\ &+\rho\sum_{p=1}^{N}\frac{2(1-s)}{\delta^{2-2s}}a\left(\zeta_{p}^{R},\zeta_{q}^{R};\hat{s}\right)_{c}u_{N}^{R}(\omega,s) \end{split}$$

$$\begin{split} -i\sum_{p=1}^{N}\sum_{m=0}^{M}\Theta_{m}^{s}(s)\frac{2(1-s)}{\delta^{2}-2s}a(\zeta_{p}^{R},\zeta_{q}^{I};s_{m})_{c}u_{N}^{R}(\omega,s) \\ -i\rho\sum_{p=1}^{N}\frac{2(1-s)}{\delta^{2}-2s}a(\zeta_{p}^{R},\zeta_{q}^{I};\hat{s})_{c}u_{N}^{R}(\omega,s) \\ +i\sum_{p=1}^{N}\sum_{m=0}^{M}\Theta_{m}^{s}(s)\frac{2(1-s)}{\delta^{2}-2s}a(\zeta_{p}^{I},\zeta_{q}^{R};s_{m})_{c}u_{N}^{I}(\omega,s) \\ +i\rho\sum_{p=1}^{N}\sum_{m=0}^{M}\Theta_{m}^{s}(s)\frac{2(1-s)}{\delta^{2}-2s}a(\zeta_{p}^{I},\zeta_{q}^{R};\hat{s})_{c}u_{N}^{I}(\omega,s) \\ +\sum_{p=1}^{N}\sum_{m=0}^{M}\Theta_{m}^{s}(s)\frac{2(1-s)}{\delta^{2}-2s}a(\zeta_{p}^{I},\zeta_{q}^{I};s_{m})_{c}u_{N}^{I}(\omega,s) \\ +\rho\sum_{p=1}^{N}\frac{2(1-s)}{\delta^{2}-2s}a(\zeta_{p}^{I},\zeta_{q}^{I};\hat{s})_{c} - \left(\hat{h}\left(\sum_{p=1}^{N}\zeta_{p}^{R}u_{N}^{R}(\omega,s)\right),\zeta_{q}^{R}\right)_{c} \\ +i\left(\hat{h}\left(\sum_{p=1}^{N}\zeta_{p}^{R}u_{N}^{R}(\omega,s)\right),\zeta_{q}^{I}\right)_{c} -i\left(\hat{h}\left(\sum_{p=1}^{N}\zeta_{p}^{I}u_{N}^{I}(\omega,s)\right),\zeta_{q}^{R}\right)_{c} \\ -\left(\hat{h}\left(\sum_{p=1}^{N}\zeta_{p}^{I}u_{N}^{I}(\omega,s)\right),\zeta_{q}^{I}\right)_{c} \\ =(\hat{f}^{R},\zeta_{q}^{R})_{c} + (\hat{f}^{I},\zeta_{q}^{I})_{c} -i(\hat{f}^{R},\zeta_{q}^{I})_{c} +i(\hat{f}^{I},\zeta_{q}^{R})_{c}. \end{split}$$

The equivalent matrix form of the above equation is

$$\begin{bmatrix}
\mathbf{M}_{1}^{\omega} + \sum_{m=0}^{M} \Theta_{m}^{s}(s) \mathbf{A}_{N}^{R} + \rho \mathbf{A}_{s}^{R} & -\mathbf{M}_{2}^{\omega} + \sum_{m=0}^{M} \Theta_{m}^{s}(s) \mathbf{A}_{N}^{I} + \rho \mathbf{A}_{s}^{I} \\
\mathbf{M}_{N}^{\omega R} - \sum_{m=0}^{M} \Theta_{m}^{s}(s) \mathbf{A}_{1} - \rho \mathbf{A}_{s1} & \mathbf{M}_{N}^{\omega I} + \sum_{m=0}^{M} \Theta_{m}^{s}(s) \mathbf{A}_{2} + \rho \mathbf{A}_{s2}
\end{bmatrix} \begin{bmatrix}
\mathbf{u}_{N}^{R} \\
\mathbf{u}_{N}^{I}
\end{bmatrix} \\
- \begin{bmatrix}
\mathbf{h}_{N}^{R} & \mathbf{h}_{N}^{I} \\
-\mathbf{h}_{1} & \mathbf{h}_{2}
\end{bmatrix} = \begin{bmatrix}
f_{N}^{R} + f_{N}^{I} \\
-f_{1} + f_{2}
\end{bmatrix},$$
(3.3)

where

$$\begin{split} \boldsymbol{M}_{N}^{\omega R}(p,q) &= \omega \left(\zeta_{p}^{R},\zeta_{q}^{R}\right)_{c'} & \boldsymbol{M}_{N}^{\omega I}(p,q) = \omega \left(\zeta_{p}^{I},\zeta_{q}^{I}\right)_{c'} \\ \boldsymbol{M}_{1}^{\omega}(p,q) &= \omega \left(\zeta_{p}^{R},\zeta_{q}^{I}\right)_{c'} & \boldsymbol{M}_{2}^{\omega}(p,q) = \omega \left(\zeta_{p}^{I},\zeta_{q}^{R}\right)_{c'} \\ \boldsymbol{A}_{N}^{R}(p,q) &= \frac{2(1-s)}{\delta^{2}-2s} a \left(\zeta_{p}^{R},\zeta_{q}^{R};s_{m}\right)_{c'} & \boldsymbol{A}_{N}^{I}(p,q) = \frac{2(1-s)}{\delta^{2}-2s} a \left(\zeta_{p}^{I},\zeta_{q}^{I};s_{m}\right)_{c'} \end{split}$$

$$\begin{split} &A_{sN}^{R}(p,q) = \frac{2(1-s)}{\delta^{2-2s}} a \left(\zeta_{p}^{R}, \zeta_{q}^{R}; \hat{s}\right)_{c}, \qquad A_{sN}^{I}(p,q) = \frac{2(1-s)}{\delta^{2-2s}} a \left(\zeta_{p}^{I}, \zeta_{q}^{I}; \hat{s}\right)_{c}, \\ &A_{1}(p,q) = \frac{2(1-s)}{\delta^{2-2s}} a \left(\zeta_{p}^{R}, \zeta_{q}^{I}; s_{m}\right)_{c}, \qquad A_{2}(p,q) = \frac{2(1-s)}{\delta^{2-2s}} a \left(\zeta_{p}^{I}, \zeta_{q}^{R}; s_{m}\right)_{c}, \\ &A_{s1}(p,q) = \frac{2(1-s)}{\delta^{2-2s}} a \left(\zeta_{p}^{R}, \zeta_{q}^{I}; \hat{s}\right)_{c}, \qquad A_{s2}(p,q) = \frac{2(1-s)}{\delta^{2-2s}} a \left(\zeta_{p}^{I}, \zeta_{q}^{R}; \hat{s}\right)_{c}, \\ &h_{N}^{R}(p,q) = \left(\hat{h}\left(\sum_{p=1}^{N} \zeta_{p}^{R} u_{N}^{R}(\omega,s)\right), \zeta_{q}^{R}\right)_{c}, \qquad h_{N}^{I}(p,q) = \left(\hat{h}\left(\sum_{p=1}^{N} \zeta_{p}^{I} u_{N}^{I}(\omega,s)\right), \zeta_{q}^{I}\right)_{c}, \\ &h_{1}(p,q) = \left(\hat{h}\left(\sum_{p=1}^{N} \zeta_{p}^{R} u_{N}^{R}(\omega,s)\right), \zeta_{q}^{I}\right)_{c}, \qquad h_{2}(p,q) = \left(\hat{h}\left(\sum_{p=1}^{N} \zeta_{p}^{I} u_{N}^{I}(\omega,s)\right), \zeta_{q}^{R}\right)_{c}, \\ &p,q = 1, \dots, N, \end{split}$$

and

$$\begin{split} f_N^R(q) &= \left(\hat{f}^R, \zeta_q^R\right)_c, \quad f_N^I(q) = \left(\hat{f}^I, \zeta_q^I\right)_c, \\ f_1(q) &= \left(\hat{f}^R, \zeta_q^I\right)_c, \quad f_2(q) = \left(\hat{f}^I, \zeta_q^R\right)_c, \quad q = 1, \dots, N. \end{split}$$

Since $\{\phi_j\}_{j=1}^{\mathcal{N}}$ is a set of the finite element basis of $V^{\mathcal{N}}$ and the basis functions $\{\zeta_j\}_{j=1}^N$ belong to the finite element space $V^{\mathcal{N}}$, we obtain

$$\zeta_p^R = \sum_{q=1}^{\mathcal{N}} Z_{pq}^R \phi_q^R, \quad \zeta_p^I = \sum_{q=1}^{\mathcal{N}} Z_{pq}^I \phi_q^I, \quad 1 \leq p \leq N.$$

Let
$$(\mathcal{Z}^R)(p,q) = Z_{pq}^R$$
 and $(\mathcal{Z}^I)(p,q) = Z_{pq}^I$, $1 \le q \le \mathcal{N}$, then

$$\begin{split} &\boldsymbol{M}_{N}^{\omega R} = (\mathcal{Z}^{R})^{T} \boldsymbol{M} \mathcal{Z}^{R}, \quad \boldsymbol{M}_{N}^{\omega I} = (\mathcal{Z}^{I})^{T} \boldsymbol{M} \mathcal{Z}^{I}, \\ &\boldsymbol{M}_{1}^{\omega} = (\mathcal{Z}^{R})^{T} \boldsymbol{M} \mathcal{Z}^{I}, \quad \boldsymbol{M}_{2}^{\omega} = (\mathcal{Z}^{I})^{T} \boldsymbol{M} \mathcal{Z}^{R}, \\ &\boldsymbol{A}_{N}^{R} = (\mathcal{Z}^{R})^{T} \boldsymbol{A}_{s_{m}} \mathcal{Z}^{R}, \quad \boldsymbol{A}_{N}^{I} = (\mathcal{Z}^{I})^{T} \boldsymbol{A}_{s_{m}} \mathcal{Z}^{I}, \\ &\boldsymbol{A}_{1} = (\mathcal{Z}^{R})^{T} \boldsymbol{A}_{s_{m}} \mathcal{Z}^{I}, \quad \boldsymbol{A}_{2} = (\mathcal{Z}^{I})^{T} \boldsymbol{A}_{s_{m}} \mathcal{Z}^{R}, \\ &\boldsymbol{A}_{s_{N}}^{R} = (\mathcal{Z}^{R})^{T} \boldsymbol{A}_{s_{m}} \mathcal{Z}^{R}, \quad \boldsymbol{A}_{s_{N}}^{I} = (\mathcal{Z}^{I})^{T} \boldsymbol{A}_{s_{m}} \mathcal{Z}^{I}, \\ &\boldsymbol{A}_{s_{1}} = (\mathcal{Z}^{R})^{T} \boldsymbol{A}_{s_{1}} \mathcal{Z}^{I}, \quad \boldsymbol{A}_{s_{2}} = (\mathcal{Z}^{I})^{T} \boldsymbol{A}_{s_{2}} \mathcal{Z}^{R}, \\ &\boldsymbol{u}_{N}^{R} = (\mathcal{Z}^{R})^{T} \boldsymbol{u}^{R}, \quad \boldsymbol{u}_{N}^{I} = (\mathcal{Z}^{I})^{T} \boldsymbol{u}^{I}, \\ &\boldsymbol{f}_{N}^{R} = (\mathcal{Z}^{R})^{T} \boldsymbol{f}^{R}, \quad \boldsymbol{f}_{N}^{I} = (\mathcal{Z}^{I})^{T} \boldsymbol{f}^{I}, \\ &\boldsymbol{f}_{1} = (\mathcal{Z}^{I})^{T} \boldsymbol{f}^{R}, \quad \boldsymbol{f}_{2} = (\mathcal{Z}^{R})^{T} \boldsymbol{f}^{I}, \end{split}$$

where $A_{s_m} = a(\phi_p, \phi_q; s_m)_c$ and $A_{\hat{s}} = a(\phi_p, \phi_q; \hat{s})_c$, $p, q = 1, ..., \mathcal{N}$. Replacing \hat{h} in (2.7) by the affine approximation \tilde{h} generated from the DEIM in Section 4.2, we get

$$H_N^R = B_N^R \Re(\hat{h}(\mathcal{Z}u_N)), \quad H_N^I = B_N^I \Im(\hat{h}(\mathcal{Z}u_N)),$$

 $H_1 = B_1 \Re(\hat{h}(\mathcal{Z}u_N)), \quad H_2 = B_2 \Im(\hat{h}(\mathcal{Z}u_N)),$

where

$$\mathbf{B}_{N}^{R} = (\mathcal{Z}^{R})^{T} \mathbf{H}_{R} (\mathbf{P}_{R}^{T} \mathbf{H}_{R})^{-1} \mathbf{H}_{R}^{T}, \quad \mathbf{B}_{N}^{I} = (\mathcal{Z}^{I})^{T} \mathbf{H}_{I} (\mathbf{P}_{I}^{T} \mathbf{H}_{I})^{-1} \mathbf{H}_{I}^{T},
\mathbf{B}_{1} = (\mathcal{Z}^{I})^{T} \mathbf{H}_{R} (\mathbf{P}_{I}^{T} \mathbf{H}_{R})^{-1} \mathbf{H}_{R}^{T}, \quad \mathbf{B}_{2} = (\mathcal{Z}^{R})^{T} \mathbf{H}_{I} (\mathbf{P}_{I}^{T} \mathbf{H}_{I})^{-1} \mathbf{H}_{I}^{T},
\mathcal{Z} = [\mathcal{Z}^{R}, \mathcal{Z}^{I}], \quad \mathbf{u}_{N} = [\mathbf{u}_{N}^{R}; \mathbf{u}_{N}^{I}].$$

Eq. (3.3) can be written as the following matrix form:

$$\begin{bmatrix}
\mathbf{M}_{1}^{\omega} + \sum_{m=0}^{M} \Theta_{m}^{s}(s) \mathbf{A}_{N}^{R} + \rho \mathbf{A}_{sN}^{R} & -\mathbf{M}_{2}^{\omega} + \sum_{m=0}^{M} \Theta_{m}^{s}(s) \mathbf{A}_{N}^{I} + \rho \mathbf{A}_{sN}^{I} \\
\mathbf{M}_{N}^{\omega R} - \sum_{m=0}^{M} \Theta_{m}^{s}(s) \mathbf{A}_{1} - \rho \mathbf{A}_{s1} & \mathbf{M}_{N}^{\omega I} + \sum_{m=0}^{M} \Theta_{m}^{s}(s) \mathbf{A}_{2} + \rho \mathbf{A}_{s2}
\end{bmatrix} \begin{bmatrix}
\mathbf{u}_{N}^{R} \\
\mathbf{u}_{N}^{I}
\end{bmatrix} \\
- \begin{bmatrix}
\mathbf{B}_{N}^{R} & \mathbf{B}_{N}^{I} \\
-\mathbf{B}_{1} & \mathbf{B}_{2}
\end{bmatrix} \begin{bmatrix}
\Re(\hat{h}(\mathcal{Z}\mathbf{u}_{N})) \\
\Im(\hat{h}(\mathcal{Z}\mathbf{u}_{N}))
\end{bmatrix} = \begin{bmatrix}
f_{N}^{R} + f_{N}^{I} \\
-f_{1} + f_{2}
\end{bmatrix}.$$
(3.4)

Based on Eq. (3.4), the offline-online decomposition is realized. In the offline phase, we only need to compute and store the *s*-independent quantities $M_N^{\omega R}$, $M_N^{\omega I}$, M_1^{ω} , M_2^{ω} , A_N^R , A_N^I , A_N^R , A_N^I ,

3.2 Posterior error

In the RB space $V_N^{\mathcal{N}}$, we use u_N to approximate $u^{\mathcal{N}}$. In order to verify the error caused by the reduction, the relevant posterior error is derived in this section. For $\forall v \in V^{\mathcal{N}}$, the residual is defined as

$$r(v;s) := (\hat{f},v)_c + (\tilde{h}(u_N(s)),v)_c - \frac{2(1-s)}{\delta^{2-2s}} \tilde{a}_{M,\rho} (u_N(s),v;s)_c - i\omega (u_N(s),v)_c.$$
(3.5)

When $v \in V_N^{\mathcal{N}}$, the residual is 0. By the Riesz representation theory, there exists $\hat{e}(s) \in V^{\mathcal{N}}$ such that

$$(\hat{e}(s),v)_{V^{\mathcal{N}}} = r(v;s), \quad \forall v \in V^{\mathcal{N}}.$$
 (3.6)

Then we introduce the dual norm of the residual

$$\epsilon_N := \sup_{v \in V^{\mathcal{N}}} \frac{r(v;s)}{\|v\|_{V^{\mathcal{N}}}} = \|\hat{e}(s)\|_{V^{\mathcal{N}}}, \tag{3.7}$$

this shall prove to be important for the offline-online stratagem developed below. The error estimator [35] for the solution is defined as

$$\Delta_N(s) = \|\hat{e}(s)\|_{V^N} / (\beta_{LB}^N(s))^{1/2},$$
 (3.8)

where

$$0 < \beta_{LB}^{\mathcal{N}}(s) \le \beta^{\mathcal{N}}(s) = \inf_{v \in V^{\mathcal{N}}} \frac{\tilde{a}_{M,\rho}(v,v;s)_c}{\|v\|_{V^{\mathcal{N}}}^2}.$$

Combining Eq. (3.5), (2.20), (2.21) and (3.2), the residual can be expressed as

$$r(v;s) := (\hat{f},v)_{c} + (\tilde{h}(u_{N}(s),v)_{c} - \tilde{a}_{M}(u_{N}(s),v;s)_{c} -\rho a(u_{N}(s),v;\hat{s})_{c} - i\omega(u_{N}(s),v)_{c} = (\hat{f},v)_{c} + \left(\tilde{h}\left(\sum_{p=1}^{N} \zeta_{p}u_{N,p}(s)\right),v\right)_{c} -\frac{2(1-s)}{\delta^{2-2s}} \sum_{p=1}^{N} \left(\sum_{m=0}^{M} \Theta_{m}^{s}(s)a(\zeta_{p},v;s_{m})_{c}u_{N,p}(s)\right) -\rho \frac{2(1-s)}{\delta^{2-2s}} \sum_{p=1}^{N} a(\zeta_{p},v;\hat{s})_{c}u_{N,p}(s) - i\omega \sum_{p=1}^{N} (\zeta_{p},v)_{c}u_{N,p}(s).$$
(3.9)

By Eqs. (3.9) and (3.6), we have

$$(\hat{e}(s),v)_{V^{N}} = (\hat{f},v)_{c} + \left(\tilde{h}\left(\sum_{p=1}^{N} \zeta_{p} u_{N,p}(s)\right),v\right)_{c}$$

$$-\frac{2(1-s)}{\delta^{2-2s}} \sum_{p=1}^{N} \left(\sum_{m=0}^{M} \Theta_{m}^{s}(s) a(\zeta_{p},v;s_{m})_{c} u_{N,p}(s)\right)$$

$$-\rho \frac{2(1-s)}{\delta^{2-2s}} \sum_{p=1}^{N} a(\zeta_{p},v;\hat{s})_{c} u_{N,p}(s) - i\omega \sum_{p=1}^{N} (\zeta_{p},v)_{c} u_{N,p}(s). \tag{3.10}$$

This implies that

$$\hat{e}(s) = \mathcal{C}_{\hat{f}} + \mathcal{C}_{\tilde{h}} + \frac{2(1-s)}{\delta^{2-2s}} \sum_{p=1}^{N} \left(\sum_{m=0}^{M} \Theta_{m}^{s}(s) u_{N,p}(s) \mathcal{L}_{s_{m}}^{p,m} \right) + \rho \frac{2(1-s)}{\delta^{2-2s}} \sum_{n=1}^{N} u_{N,p}(s) \mathcal{L}_{\hat{s}}^{p} + i\omega \sum_{n=1}^{N} u_{N,p}(s) \mathcal{X}^{p},$$
(3.11)

where $C_{\hat{f}}$ and $C_{\tilde{h}}$ are the Riesz representations of $(\hat{f},v)_c$ and $(\tilde{h},v)_c$, respectively, i.e.,

$$(\mathcal{C}_{\hat{f}},v)_{V^{\mathcal{N}}}=(\hat{f},v)_{c}, \quad (\mathcal{C}_{\tilde{h}},v)_{V^{\mathcal{N}}}=(\tilde{h},v)_{c}, \quad \forall v \in V^{\mathcal{N}}.$$

Let $\mathcal{L}^{p,m}_{s_m}$ and \mathcal{L}^p_s be the Riesz representations of $a(\zeta_p,v;s_m)_c$ and $a(\zeta_p,v;\hat{s})_c$, respectively, i.e.,

$$(\mathcal{L}_{s_m}^{p,m},v)_{V\mathcal{N}} = -a(\zeta_p,v;s_m)_c, \quad (\mathcal{L}_{\hat{s}}^p,v)_{V\mathcal{N}} = -a(\zeta_p,v;\hat{s})_c, \quad \forall v \in V^{\mathcal{N}},$$

where $1 \le p \le N$ and $0 \le m \le M$. Assume that \mathcal{X}^p is the Riesz representation of $(\zeta_p, v)_c$, i.e.,

$$(\mathcal{X}^p, v)_{V^{\mathcal{N}}} = -(\zeta_p, v)_c.$$

Then Eq. (3.11) can be written as

$$\begin{split} \left\| \hat{e}(s) \right\|_{V^{\mathcal{N}}}^{2} &= (\mathcal{C}_{\hat{f}}, \mathcal{C}_{\hat{f}})_{V^{\mathcal{N}}} + 2(\mathcal{C}_{\hat{f}}, \mathcal{C}_{\tilde{h}})_{V^{\mathcal{N}}} + \frac{4(1-s)}{\delta^{2-2s}} \sum_{p=1}^{N} \sum_{m=0}^{M} \Theta_{m}^{s}(s) u_{N,p}(s) \left(\mathcal{C}_{\hat{f}}, \mathcal{L}_{s_{m}}^{p,m}\right)_{V^{\mathcal{N}}} \\ &+ \rho \frac{4(1-s)}{\delta^{2-2s}} \sum_{p=1}^{N} u_{N,p}(s) \left(\mathcal{C}_{\hat{f}}, \mathcal{L}_{s}^{p}\right)_{V^{\mathcal{N}}} \\ &+ (\mathcal{C}_{\tilde{h}}, \mathcal{C}_{\tilde{h}})_{V^{\mathcal{N}}} + \frac{4(1-s)}{\delta^{2-2s}} \sum_{p=1}^{N} \sum_{m=0}^{M} \Theta_{m}^{s}(s) u_{N,p}(s) \left(\mathcal{C}_{\tilde{h}}, \mathcal{L}_{s_{m}}^{p,m}\right)_{V^{\mathcal{N}}} \\ &+ \rho \frac{4(1-s)}{\delta^{2-2s}} \sum_{p=1}^{N} u_{N,p}(s) \left(\mathcal{C}_{\tilde{h}}, \mathcal{L}_{s}^{p}\right)_{V^{\mathcal{N}}} \\ &+ \frac{4(1-s)^{2}}{\delta^{4-4s}} \sum_{p=1}^{N} \sum_{p'=1}^{N} \sum_{m=0}^{M} \sum_{m'=0}^{M} \Theta_{m}^{s}(s) u_{N,p}(s) \Theta_{m'}^{s}(s) u_{N,p'}(s) \left(\mathcal{L}_{s_{m}}^{p,m}, \mathcal{L}_{s_{m'}}^{p',m'}\right)_{V^{\mathcal{N}}} \\ &+ \rho \frac{8(1-s)^{2}}{\delta^{4-4s}} \sum_{p=1}^{N} \sum_{p'=1}^{N} \sum_{m=0}^{M} \Theta_{m}^{s}(s) u_{N,p}(s) u_{N,p'}(s) \left(\mathcal{L}_{s_{m}}^{p,m}, \mathcal{L}_{s}^{p'}\right)_{V^{\mathcal{N}}} \\ &+ \rho^{2} \frac{4(1-s)^{2}}{\delta^{4-4s}} \sum_{p=1}^{N} \sum_{r'=1}^{N} u_{N,p}(s) u_{N,p'}(s) \left(\mathcal{L}_{s}^{p}, \mathcal{L}_{s}^{p'}\right)_{V^{\mathcal{N}}} \end{split}$$

$$+\omega^{2} \sum_{p=1}^{N} \sum_{p'=1}^{N} u_{N,p}(s) u_{N,p'}(s) (\mathcal{X}^{p}, \mathcal{X}^{p'})_{V^{\mathcal{N}}}.$$
 (3.12)

To efficiently compute $\|\hat{e}(s)\|_{V^N}$ and Δ_N , we apply an offline-online procedure. In the offline phase, we compute and store the quantities independent of the uncertainties. In particular, we compute $\mathcal{C}_{\hat{f}}, \mathcal{C}_{\tilde{h}}, \mathcal{L}_{s_m}^{p,m}, \mathcal{L}_{\hat{s}}^p$ and \mathcal{X}^p , and store

$$(\mathcal{C}_{\hat{f}}, \mathcal{C}_{\hat{f}})_{V^{\mathcal{N}}}, (\mathcal{C}_{\hat{f}}, \mathcal{C}_{\tilde{h}})_{V^{\mathcal{N}}}, (\mathcal{C}_{\hat{f}}, \mathcal{L}_{s_{m}}^{p,m})_{V^{\mathcal{N}}}, (\mathcal{C}_{\hat{f}}, \mathcal{L}_{\hat{s}}^{p})_{V^{\mathcal{N}}}, (\mathcal{C}_{\tilde{h}}, \mathcal{C}_{\tilde{h}})_{V^{\mathcal{N}}}, (\mathcal{C}_{\tilde{h}}, \mathcal{L}_{s_{m}}^{p,m})_{V^{\mathcal{N}}}, (\mathcal{C}_{\tilde{h}}, \mathcal{L}_{s_{m}}^{p,m})_{V^{\mathcal{N}}}, (\mathcal{L}_{s_{m}}^{p,m}, \mathcal{L}_{s_{m}}^{p'})_{V^{\mathcal{N}}}, (\mathcal{L}_{\hat{s}}^{p}, \mathcal{L}_{\hat{s}}^{p'})_{V^{\mathcal{N}}}, (\mathcal{L}_{\hat{s}}^{p}, \mathcal{L}_{\hat{s}}^{p'})_{V^{\mathcal{N}}}, (\mathcal{L}_{r}^{p}, \mathcal{L}_{r}^{p'})_{V^{\mathcal{N}}}, (\mathcal{L}_{r}^{p}, \mathcal{L}_{r}^{p'}, \mathcal{L}_{r}^{p'})_{V^{\mathcal{N}}}, (\mathcal{L}_{r}^{p}, \mathcal{L}_{r}^{p'}, \mathcal{L}_{r}^{p'}, \mathcal{L}_{r}^{p'}, \mathcal{L}_{r}^{p'})_{V^{\mathcal{N}}}, (\mathcal{L}_{r}^{p}, \mathcal{L}_{r}^{p'}, \mathcal{L}_{r$$

where $1 \le p, p' \le N$, $0 \le m, m' \le M$. In the online phase, for $\forall s$, we compute $u_{N,p} (1 \le p \le N)$, and use Eqs. (3.12) and (3.8) to compute $\|\hat{e}(s)\|_{V^N}$ and Δ_N , respectively.

4 Sampling strategy

The choice of the RB affects the accuracy of the approximation. In this paper, a common observation is used to construct a set of basis functions, i.e., the solution space is often attracted to a low-dimensional manifold for a particular system. Here two sampling processes are needed. The first is to construct the affine space of the nonlinear term and the second is to construct a RB space $V_N^{\mathcal{N}}$ using the MOS-greedy algorithm. Thus, the proposed sampling method combines the MOS for ω with the greedy procedure for s. We will briefly review the algorithms that are used in the process.

4.1 Method of snapshots

POD has been used in many applications to construct low-rank subspaces, which retain most of the energy presented in all original variables. One of the most important properties of POD is that an optimal approximation is constructed in the least squares sense. Given a set of snapshots $\{\hat{u}^{\mathcal{N}}(\omega_1,s),\hat{u}^{\mathcal{N}}(\omega_2,s),\cdots,\hat{u}^{\mathcal{N}}(\omega_{N_t},s)\}$ $\subset \mathbb{R}^{\mathcal{N}}$, let the sets of the real- and imaginary-part of snapshots separately, i.e.,

$$\mathbf{X}^{R} := \left\{ \Re \left(\hat{u}^{\mathcal{N}}(\omega_{j}, s) \right) \right\}_{j=1}^{N_{t}}, \quad \mathbf{X}^{I} := \left\{ \Im \left(\hat{u}^{\mathcal{N}}(\omega_{j}, s) \right) \right\}_{j=1}^{N_{t}}.$$

For the real snapshots

$$\boldsymbol{X}^{R} := \left\{ \Re \left(\hat{u}^{\mathcal{N}}(\omega_{j}, s) \right) \right\}_{i=1}^{N_{t}} = \left\{ X_{j}^{R} \right\}_{i=1}^{N_{t}},$$

we approximate snapshot X_i^R by using a set of orthogonal vectors

$$\mathbf{\Psi}^{R} = \left\{ \psi_{1}^{R}, \psi_{2}^{R}, \cdots, \psi_{N}^{R} \right\} \subset \mathbb{R}^{\mathcal{N}}$$

with rank $N < \mathcal{N}$. Then, the approximation is given by

$$X_j^R \approx \sum_{p=1}^N x_p^j \psi_p^R, \quad j=1,...,N_t.$$

The above approximation is also equivalent to

$$X_j^R \approx \mathbf{\Psi}^R(\mathbf{\Psi}^R)^T X_j^R, \quad j=1,...,N_t.$$

From reference [34], it can be seen that the POD basis is provided by SVD of X^R ,

$$X^R = U^R \Sigma^R (\mathbf{Y}^R)^T$$

where $\boldsymbol{U}^R = [U_1^R, \cdots, U_{n_r}^R] \in \mathbb{R}^{N \times n_r}$, $\boldsymbol{Y}^R = [Y_1^R, \cdots, Y_{n_r}^R] \in \mathbb{R}^{N_t \times n_r}$ and $\boldsymbol{\Sigma}^R = \operatorname{diag}(\sigma_1^R, \cdots, \sigma_{n_r}^R) \in \mathbb{R}^{n_r \times n_r}$. The set of the first N ($N \le n_r$) left singular vectors U_1^R, \cdots, U_N^R from \boldsymbol{U}^R is chosen as the POD basis $\boldsymbol{\Psi}^R$. The error between the snapshots and the corresponding POD solutions is as follows:

$$\sum_{j=1}^{N_t} ||X_j^R - \mathbf{\Psi}^R (\mathbf{\Psi}^R)^T X_j^R||_2^2 = \sum_{l=N+1}^{n_r} (\sigma_l^R)^2.$$
 (4.1)

In most cases, the snapshot matrix is overdetermined, indicating more degrees of freedom than snapshots. Directly performing the SVD for the matrix is expensive. To reduce costs, a technique called the method of snapshots (MOS) is often used. Given a set of snapshots

$$\mathbf{X}^R := \left\{ \Re \left(\hat{u}^{\mathcal{N}}(\omega_j, s) \right) \right\}_{j=1}^{N_t},$$

we compute the covariance matrix K^R , where

$$\boldsymbol{K}_{p,q}^{R} := \left(\Re\left(\hat{u}^{\mathcal{N}}(\omega_{p},s)\right),\Re\left(\hat{u}^{\mathcal{N}}(\omega_{q},s)\right)\right)_{c} = (\boldsymbol{X}^{R})^{T}\boldsymbol{X}^{R}.$$

By using the SVD of X^R , we have

$$\mathbf{K}^R = (\mathbf{U}^R \Sigma^R (\mathbf{Y})^R)^T (\mathbf{U}^R \Sigma^R \mathbf{Y}^R) = \mathbf{Y}^R (\Sigma^R)^2 (\mathbf{Y}^R)^T \Leftrightarrow \mathbf{K}^R \mathbf{Y}^R = \mathbf{Y}^R (\Sigma^R)^2.$$

Thus, the eigenvector of K^R correspond to the right singular vectors of X^R , and the eigenvalue of K^R correspond to the square of singular value for X^R , respectively. Let $\{\lambda_p, e_p\}$ be the normalized eigen-pairs of K^R , $1 \le p \le N_t$. Setting $(e_p)_j = e_p^j$, the k-th MOS basis function is given by

$$\psi_p(s) := \frac{1}{\sqrt{\lambda_p}} \sum_{j=1}^{N_t} e_p^j \Re \left(\hat{u}^{\mathcal{N}}(\omega_j, s) \right) = \frac{1}{\sqrt{\lambda_p}} \sum_{j=1}^{N_t} (\boldsymbol{e}_p)_j \boldsymbol{X}_j^R.$$

It is easy to get $(\psi_p, \psi_l)_V = \delta_{p,l}$, $1 \le p, l \le N_t$. Then it holds that

$$\Re(\hat{u}^{\mathcal{N}}(\omega,s)) \approx \sum_{j=1}^{N_t} \sqrt{\lambda_j} \varrho_j(\omega) \psi_j(s),$$

where $\{\varrho_j(\omega)\}_{j=1}^{N_t}$ are given by

$$\varrho_{j}(\omega) := \frac{1}{\sqrt{\lambda_{j}}} \Big(\Re \big(\hat{u}^{\mathcal{N}}(\omega, \cdot) \big), \psi_{j} \Big)_{c}.$$

Thus, we get the decomposition

$$\Re\left(\hat{u}^{\mathcal{N}}(\omega_{j},s)\right) \approx \sum_{i=1}^{N} \sqrt{\lambda_{j}} \varrho_{j}(\omega) \psi_{j}(s).$$

The steps for constructing a MOS basis matrix are summarized in Algorithm 1.

Algorithm 1: MOS Algorithm.

Input: Snapshots $\{\hat{u}^{\mathcal{N}}(\omega_1,s),\hat{u}^{\mathcal{N}}(\omega_2,s),\cdots,\hat{u}^{\mathcal{N}}(\omega_{N_t},s)\}\in\mathbb{R}^{\mathcal{N}},N_t\leq\mathcal{N}$ and MOS dimension N.

Output: MOS basis matrix $\mathbf{\Psi}^R = [\psi_1^R, \dots, \psi_N^R]$ and $\mathbf{\Psi}^I = [\psi_1^I, \dots, \psi_N^I] \in \mathbb{R}^{N \times N}$.

1 Take the real part and the imaginary part of the snapshots

$$\mathbf{X}^{R} := \{ \Re(\hat{u}^{\mathcal{N}}(\omega_{j}, s)) \}_{i=1}^{N_{t}}, \quad \mathbf{X}^{I} := \{ \Im(\hat{u}^{\mathcal{N}}(\omega_{j}, s)) \}_{i=1}^{N_{t}}.$$

- ² Compute covariance matrix $\mathbf{K}^R = (\mathbf{X}^R)^T \mathbf{X}^R$, $\mathbf{K}^I = (\mathbf{X}^I)^T \mathbf{X}^I$.
- 3 Calculate eigen-decomposition $\boldsymbol{K}^R = \boldsymbol{Y}^R \boldsymbol{D}^R (\boldsymbol{Y}^R)^T$, $\boldsymbol{K}^I = \boldsymbol{Y}^I \boldsymbol{D}^I (\boldsymbol{Y}^I)^T$, where $\boldsymbol{D}^R = \operatorname{diag}((\sigma_1^R)^2, \cdots, (\sigma_{n_r}^R)^2)$, $\boldsymbol{D}^I = \operatorname{diag}((\sigma_1^I)^2, \cdots, (\sigma_{n_r}^I)^2)$.
- 4 Construct the MOS basis matrix

Construct the MOS basis matrix
$$\mathbf{Y}^R = \mathbf{X}^R \mathbf{Y}_N^R (\mathbf{D}_N^R)^{-1/2}, \quad \mathbf{Y}^I = \mathbf{X}^I \mathbf{Y}_N^I (\mathbf{D}_N^I)^{-1/2},$$
 where $\mathbf{Y}_N^R = \mathbf{Y}^R (:,1:N), \mathbf{D}_N^R = \mathbf{D}^R (1:N,1:N), \mathbf{Y}_N^I = \mathbf{Y}^I (:,1:N)$ and $\mathbf{D}_N^I = \mathbf{D}^I (1:N,1:N).$

4.2 Affine forms of nonlinear terms

It is computationally inefficient to directly use the nonlinear terms obtained from the MOS method to reduce order solution, and the computational complexity of the nonlinear term depends on the dimension of the full order system. To overcome the difficulty, an effective way is to approximate the nonlinear function by projecting it onto a subspace. The subspace is spanned by a basis of dimension $Q \ll \mathcal{N}$ [9]. By projecting a nonlinear function $\hat{h}: s \in \mathcal{P}^s \to \hat{h}(u(x,\omega,s)) \in \mathbb{R}^{\mathcal{N}}$ onto a subspace spanned by a basis H, the approximation

$$\hat{h}(\mathbf{u}(\omega,s),\omega,s) \approx \tilde{h}(\mathbf{u}(\omega,s),\omega,s) = \mathbf{H} \cdot \mathbf{c}(\omega,s),$$
 (4.2)

where $\mathbf{H} = [h_1, \cdots, h_Q] \in \mathbb{R}^{\mathcal{N} \times \mathcal{Q}}$. This basis function is generated by sampling the evaluation of snapshots $\hat{h}(\hat{u}^{\mathcal{N}}(\omega, s))$ at values s^i_{DEIM} $(i = 1, \dots, N_Q \ (N_Q > Q))$ and then calculating the Q modes by the SVD of these snapshots. Here $\mathbf{c}(\omega, s) \in \mathbb{R}^Q$ is the corresponding vector of coefficients that can be uniquely determined by

$$\mathbf{P}^{T}\widetilde{h}(\mathbf{u}(\omega,s),\omega,s) = (\mathbf{P}^{T}\mathbf{H})\mathbf{c}(\omega,s), \tag{4.3}$$

where $P = \{e_{\wp_1}, \cdots, e_{\wp_Q}\} \in \mathbb{R}^{\mathcal{N} \times Q}$ and $e_{\wp_i} = [0, \cdots, 0, 1, 0, \cdots, 0] \in \mathbb{R}^{\mathcal{N}}$ is the \wp_i -th column of the identity matrix $I \in \mathbb{R}^{\mathcal{N} \times \mathcal{N}}$ $(i = 1, \dots, Q)$. Suppose that $P^T H$ is nonsingular. Then the coefficient vector $c(\omega, s)$ can be determined uniquely by Eq. (4.3) and the final approximation form (4.2) becomes

$$\widetilde{h}(\mathbf{u}(\omega,s),\omega,s) = \mathbf{H} \cdot \mathbf{c}(\omega,s) = \mathbf{H}(\mathbf{P}^T \mathbf{H})^{-1} \mathbf{H}^T \widehat{h}(\mathbf{u}(\omega,s),\omega,s). \tag{4.4}$$

To obtain the approximation (4.4), we must specify

- 1. the projection basis $\{h_1, \dots, h_Q\}$,
- 2. the interpolation indices $\{\wp_1, \dots, \wp_Q\}$ used in P.

The construction of the basis and the selection of interpolation points are summarized in Algorithm 2. In practice, the number of iterations Q typically results in a sufficiently small error ε_{DEIM} . So we can ignore the interpolation errors between \hat{h} and \tilde{h} in the subsequent process.

Remark 4.1. The DEIM is suitable for nonlinear forms with explicit expressions. However, in this paper, the Fourier transform in time is employed. The nonlinear terms may not have an explicit expression depending on the frequency solution $\hat{u}(\omega)$. To address this, data interpolation is necessary to map the nonlinear time-dependent discrete data to frequency-dependent data points. Consequently, the

Algorithm 2: DEIM Algorithm.

```
Input: A set of snapshots \mathbf{Z}^R := \{\hat{h}(\Re(\hat{u}^N(\omega,s_i)))\}_{i=1}^{N_Q} \subset \mathbb{R}^N, \mathbf{Z}^I := \{\hat{h}(\Im(\hat{u}^N(\omega,s_i)))\}_{i=1}^Q \subset \mathbb{R}^N. Output: A set of indicators \vec{\wp}^R = [\wp_1^R, \cdots, \wp_Q^R]^T, \vec\wp^I = [\wp_1^I, \cdots, \wp_Q^I]^T \in \mathbb{R}^Q.

1 Compute a set of linearly independent basis \{h_i^R, h_i^I, 1 \le i \le Q\} = MOS(\mathbf{Z}^R, \mathbf{Z}^I, Q);

2 [\sim, \wp_1^R] = \max\{|h_1^R|\}, [\sim, \wp_1^I] = \max\{|h_1^I|\};

3 \mathbf{H}_R = [h_1^R], \mathbf{P}_R = [\mathbf{e}_{\wp_1^R}], \vec\wp^R = [\wp_1^R]; \mathbf{H}_I = [h_1^I], \mathbf{P}_I = [\mathbf{e}_{\wp_I^I}], \vec\wp^I = [\wp_1^I];

4 \mathbf{for} \ i = 2 : Q \ \mathbf{do}

5 | \text{Solve} \ (\mathbf{P}_R^T \mathbf{H}_R) \mathbf{c}^R = \mathbf{P}_R^T h_i^R, \ (\mathbf{P}_I^T \mathbf{H}_I) \mathbf{c}^I = \mathbf{P}_I^T h_i^I \ \text{for} \ \mathbf{c}^R \ \text{and} \ \mathbf{c}^I;

6 \mathbf{r}^R = h_i^R - \mathbf{H}_R \mathbf{c}^R, \ \mathbf{r}^I = h_i^I - \mathbf{H}_I \mathbf{c}^I;

7 [\sim, \wp_i^R] = \max\{|\mathbf{r}^R|\}, \ [\sim, \wp_i^I] = \max\{|\mathbf{r}^I|\};

8 \mathbf{H}_R \leftarrow [\mathbf{H}_R \ h_i^R], \ \mathbf{P}_R \leftarrow [\mathbf{P}_R \ \mathbf{e}_{\wp_i^R}^R], \ \vec\wp^R \leftarrow \begin{bmatrix} \vec\wp^R \\ \wp_i^R \end{bmatrix}, \ \mathbf{H}_I \leftarrow [\mathbf{H}_I \ h_i^I],

9 \mathbf{end}
```

resulting discrete solution is parameter-dependent. To obtain the affine form of Eq. (4.2), we employ the Chebyshev interpolation in Section 2.4. Since the non-linear term does not require coercive, unlike bilinear forms, a regularization term is unnecessary. The separation form of the nonlinear terms is as follows:

$$\hat{h} \approx \widetilde{h}_M := \sum_{m=0}^M \Theta_m^s(s) \hat{h} \left(\hat{u}(\omega, s_m), \omega, s_m \right), \quad \Theta_m^s(s) := \prod_{\substack{j=0 \ j \neq m}} \frac{s - s_j}{s_m - s_j}. \tag{4.5}$$

4.3 MOS-greedy algorithm

The goal of this paper is to employ the MOS-greedy algorithm to select the basis function and perform model reduction. To initialize the MOS-greedy sampling procedure, we define a training set Ξ_{train} and an initial sample s_0 . The cardinality of Ξ_{train} is denoted by $|\Xi_{\text{train}}| = n_{\text{train}}$. The algorithm depends on two suitable integers N_1 and N_2 . The detailed procedure is described in Algorithm 3.

As described in Section 3.2, Δ_N provides a cheap posteriori error bound for $||u^N - u_N||$. In the above process, we can also set the desired error tolerance ϵ_{tol}

Algorithm 3: MOS-greedy Algorithm.

Input: A training set Ξ_{train} and snapshots $X^R, X^I, s_0 \in \Xi_{\text{train}}, N_1, N_2$.

Output: The RB approximation spaces

$$V_N^{\mathcal{N}} = \operatorname{span}\{\zeta_j^R, \zeta_j^I, 1 \le j \le N\}, 1 \le N \le N_{\max}.$$

- 1 Initialize $n=1, \mathcal{Y}^R = \emptyset, \mathcal{Y}^I = \emptyset, s_n = s_0.$
- ² Compute the optimal basis functions with regard to different frequency levels $\{\psi_j^R, \psi_j^I, 1 \le j \le N_1\} = MOS(X^R, X^I, N_1)$ by Algorithm 1.
- 3 Update $\mathcal{Y}^R \leftarrow \{\mathcal{Y}^R, \{\psi_j^R, 1 \leq j \leq N_1\}\}, \mathcal{Y}^I \leftarrow \{\mathcal{Y}^I, \{\psi_j^I, 1 \leq j \leq N_1\}\}, N \leftarrow N + N_2.$
- 4 Construct the RB approximation spaces via MOS algorithm again, i.e., $\{\zeta_j^R, \zeta_j^I, 1 \le j \le N\} = \text{MOS}(\mathcal{Y}^R, \mathcal{Y}^I, N)$.
- 5 Update Ξ_{train} with $\Xi_{\text{train}} \leftarrow \Xi_{\text{train}} = \Xi_{\text{train}} \setminus s_n$, for each $s \in \Xi_{\text{train}}$, evaluate the error Δ_N by (3.8).
- 6 Choose $s_{n+1} = \underset{s \in \Xi_{\text{train}}}{\operatorname{argmin}} \Delta_N$, and set $er_n = \underset{s \in \Xi_{\text{train}}}{\operatorname{max}} \Delta_N$.
- 7 $n \leftarrow n+1$.
- 8 Return to Step 2 if $er_n \le er_{n-1}$, otherwise terminate.

and stop the procedure when $\Delta_N \leq \epsilon_{\mathrm{tol}}$. The selection of N_1 satisfies the internal MOS error criterion, which is based on the sum of the usual eigenvalues and ϵ_{tol} . The choice of $N_2 \leq N_1$ is to minimize repetition in the RB space. It should be noted that the MOS-greedy algorithm easily selects duplicate s_n in continuous greedy cycles. Therefore, in the MOS-greedy algorithm, we delete the parameters that have already been selected. In this paper, MOS operates on one (frequency) dimension, and the greedy explores other (parameter) dimensions. Therefore, for large parameter domains and a wide range of parameter training samples, this process is still computationally feasible. Compared to the standard MOS algorithm, which requires computing FEM solutions for all training samples, the MOS-greedy algorithm computes significantly fewer FEM snapshots due to the greedy iteration, enabling rapid and uniform convergence across the parameter domain.

During the MOS-greedy sampling procedure, the best approximation h of h is employed to minimize errors from the discrete empirical interpolation. In order to clearly illustrate the proposed method, the algorithm is summarized in the flowchart shown in Fig. 2.

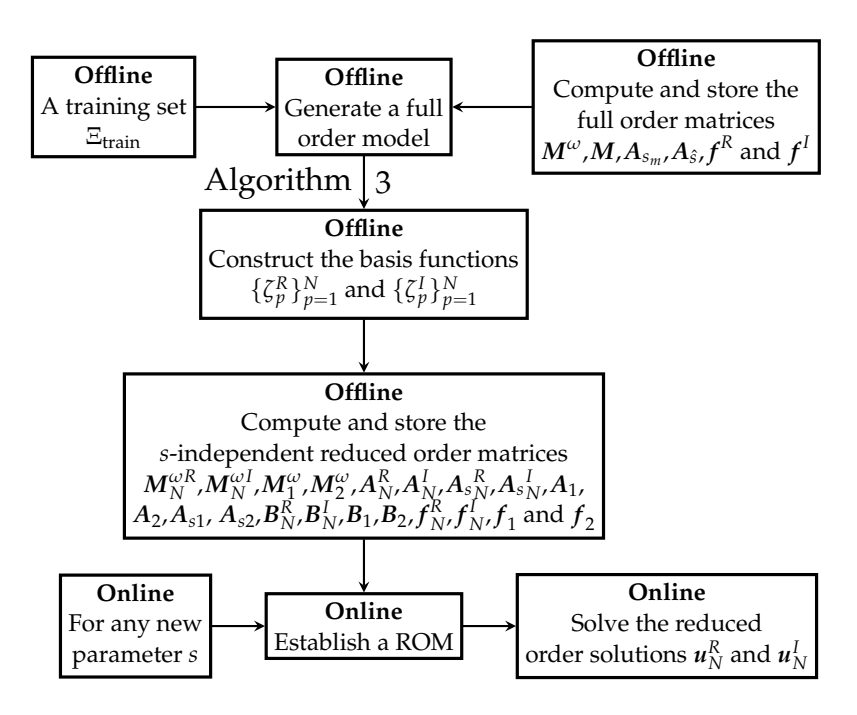


Figure 2: Flowchart of MOS-greedy method.

5 Numerical results

We demonstrate the effectiveness of the proposed MOS-greedy algorithm through two numerical examples for solving nonlocal diffusion models. In Section 5.1, we address a nonhomogeneous nonlocal heat equation with random inputs. In Section 5.2, we solve a parameterized nonlocal reaction-diffusion equation. Here, we only considered the error caused by the RB approximation. The error of the finite element discretization and Fourier transform is not considered, where more details can be found in [5,31].

For the computational domain in this paper, spatial domain $\Omega = (0,1)$. The other model parameters used are set as

$$\delta = 1/8$$
, $\Delta x = 1/128$, $\Delta t = 0.001$, $T = 1$, $M = 32$, $n_t = |\Xi_{\text{train}}| = 20$.

Let \hat{u}_N be the solutions of the proposed MOS-greedy algorithm, and \hat{u}^N be the reference (full order) solutions, which are solved by FEM. Then the relative mean error in the weighted L^2 norm is defined as

$$error = \frac{1}{\mathfrak{N}} \sum_{i=1}^{\mathfrak{N}} \frac{\|\hat{u}_N(x,\omega;s_i) - \hat{u}^{\mathcal{N}}(x,\omega;s_i)\|^2}{\|\hat{u}^{\mathcal{N}}(x,\omega;s_i)\|^2},$$
(5.1)

where \mathfrak{N} is the number of samples.

5.1 Nonhomogeneous nonlocal heat equation with random inputs

In this numerical example, we consider a nonhomogeneous nonlocal heat Eq. (2.1) with h = 0. Here $\mathcal{P}^s = [1/3,157/300]$ and the true analysis solution

$$u(x,t,s) = (s(x^2-x^4)+s^2(x^3-x^5)) \exp(-t^2).$$

Using the Fourier transform for u(x,t,s),

$$\hat{u}(x,\omega,s) = \sqrt{\pi} (s(x^2 - x^4) + s^2(x^3 - x^5)) \exp\left(-\frac{\omega^2}{4}\right).$$

Then the right hand-side can be derived as

$$\hat{f}(x,\omega,s) = -i\sqrt{\pi}\omega \left(s(x^2 - x^4) + s^2(x^3 - x^5)\right) \exp\left(-\frac{\omega^2}{4}\right) + \sqrt{\pi}\left(20x^3 + 12x^2 - 6x - 2 + (5x + 1)\frac{2s - 2}{s - 2}\delta^2\right) \exp\left(-\frac{\omega^2}{4}\right).$$

In addition, we have a homogeneous initial condition, and the volume constraint is given by

$$\hat{g}(x,\omega,s) = \hat{u}(x,\omega,s), \quad x \in [-\delta,0] \cup [1,1+\delta].$$

In this example, $\omega^* = 4.87$, $N_{\omega} = 6$, $N_1 = 5$ and $N_2 = 4$. 1000 samples are used in Algorithm 3 to construct the RB approximation spaces. To assess the accuracy of the reduced order solution, we compare the mean of the reference solution and the reduced order solution (with 6 basis functions) across 1000 samples, as shown in Fig. 3 (left). It shows the reduced order solution is a good approximation of the reference solution. Fig. 3 (right) further illustrates the reduced order solution for varying parameters, revealing a nontrivial parameter dependency.

We randomly choose 1000 samples and compute the average relative errors defined as Eq. (5.1). The average relative error against the number of the basis functions is shown in Fig. 4 (left). Additionally, Fig. 4 (right) plots the average relative errors versus different time levels for N = 2,4,10. By Fig. 4 (left), we find that the average relative error decreases when the number of the basis functions N increases. To further demonstrate the effectiveness of the proposed method, we plot the means and variances of the reference and reduced order solution in Fig. 5. To construct the ROM, the number of basis functions is N = 6. From this figure, we find that the mean and variance profiles for the reference and reduced order solutions are almost identical. This shows that the proposed MOS-greedy method can provide a good approximation for the nonlocal problems with random inputs.

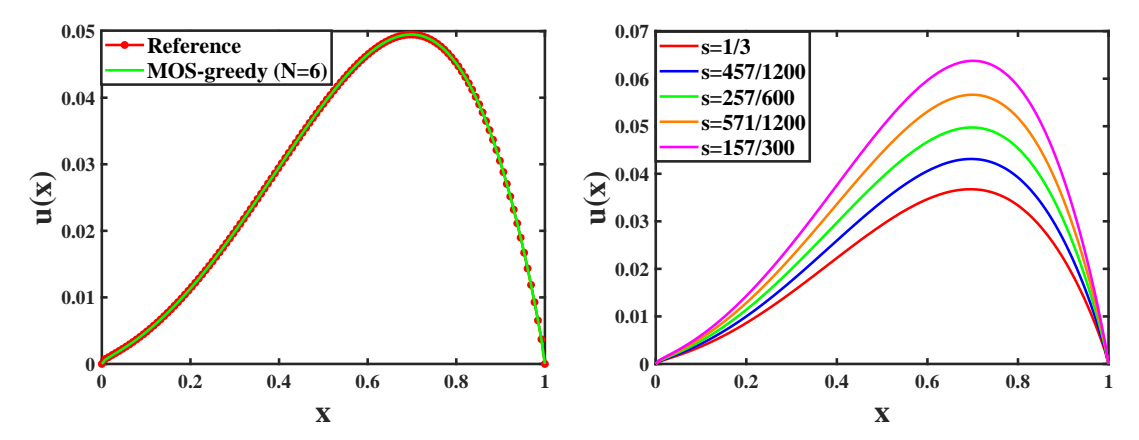


Figure 3: The mean of the reference and reduced order solution with N=6 (left) and reduced order solutions with different parameters (right).

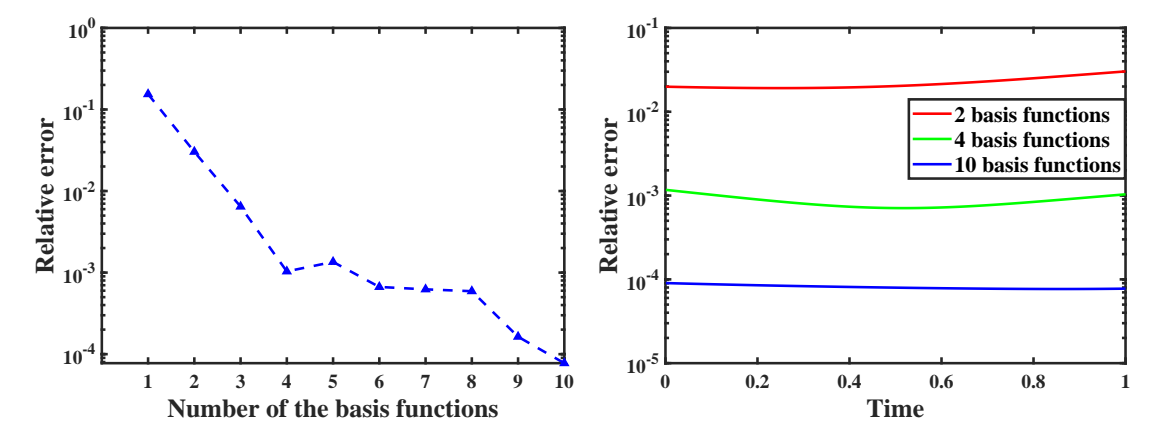


Figure 4: The average relative error against the number of the basis functions (left) and the average relative error versus different time levels for N=2,4,10.

5.2 Nonlocal reaction-diffusion equation with nonlinear terms

In this numerical example, we consider the nonlocal reaction-diffusion model (2.1) with $h(u,t,s)=u-u^3$. For this example, $\mathcal{P}^s=[1/3,1/2]$ and the exact solution

$$u(x,t,s) = s\sin\left(2\pi\left(x + \frac{3}{2}\right)\right)t\exp(-t^2).$$

After the Fourier transform,

$$\hat{u}(x,\omega,s) = -i\frac{\sqrt{\pi}}{2}s\sin\left(2\pi\left(x+\frac{3}{2}\right)\right)\omega\exp\left(-\frac{\omega^2}{4}\right).$$

We set $\omega^* = 1.23$, $N_{\omega} = 5$, $N_1 = 5$, $N_2 = 3$ and choose 1000 samples.

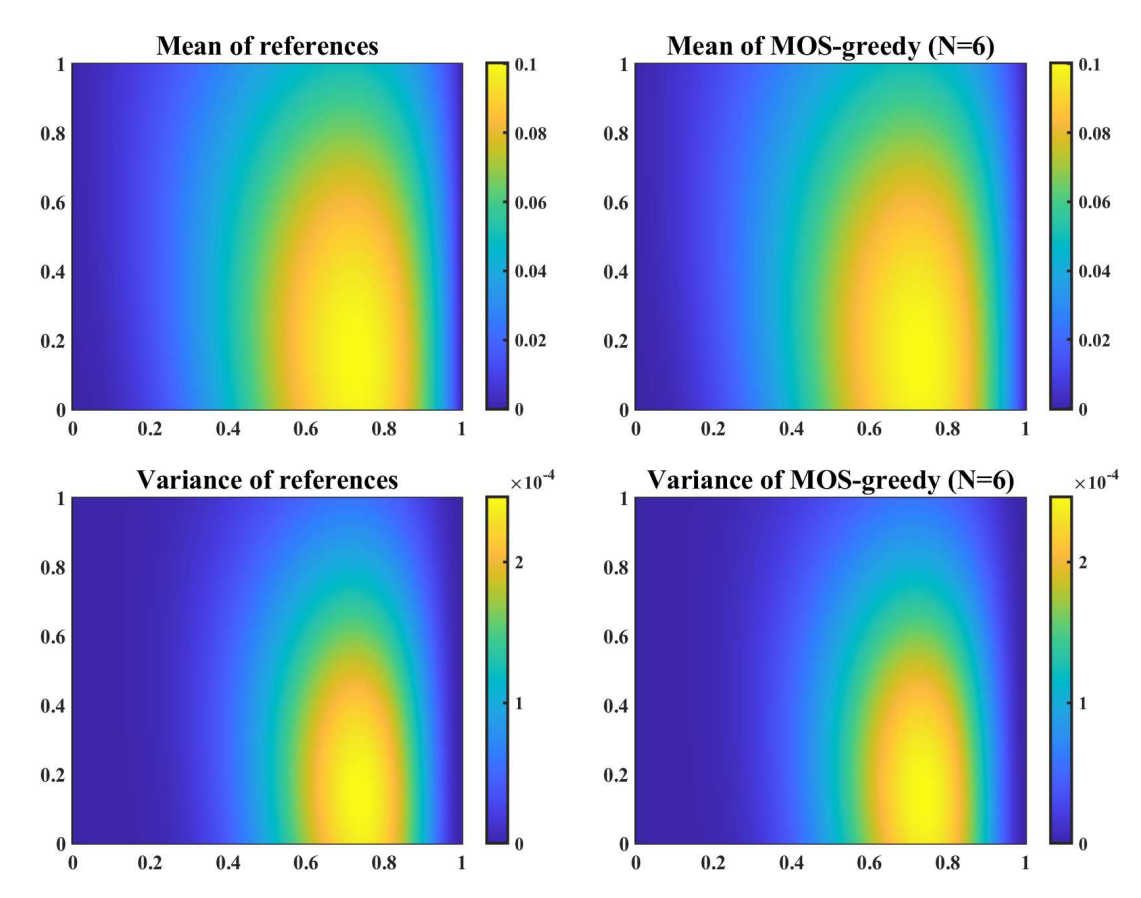


Figure 5: The mean and variance of the reference and reduced order solution with N=6. The first row is the mean profiles and the second row is the variance profiles.

Here the nonlinear term does the Fourier transform with respect to time and lacks an explicit representation in terms of $\hat{u}(\omega)$. Consequently, data interpolation is required to map the time-dependent nonlinear discrete data to frequency-dependent data points. This results in a parameter-dependent discrete solution. In this case, the nonlinear term is treated similarly with bilinear to obtain the affine form (4.5).

For this example, we present the results as shown in Figs. 6-8. Fig. 6 (left) shows the mean of the reference and reduced order solutions, computed using 6 basis functions for the nonlinear diffusion problem across 1000 samples. Fig. 6 (right) displays the reduced order solutions of (3.4) for varying parameters *s*, demonstrating the method's ability to provide efficient and accurate approximations for nonlocal problems with nonlinear terms.

To visualize the relative errors against the number of basis functions, we plot the average relative error corresponding to the different numbers of the basis

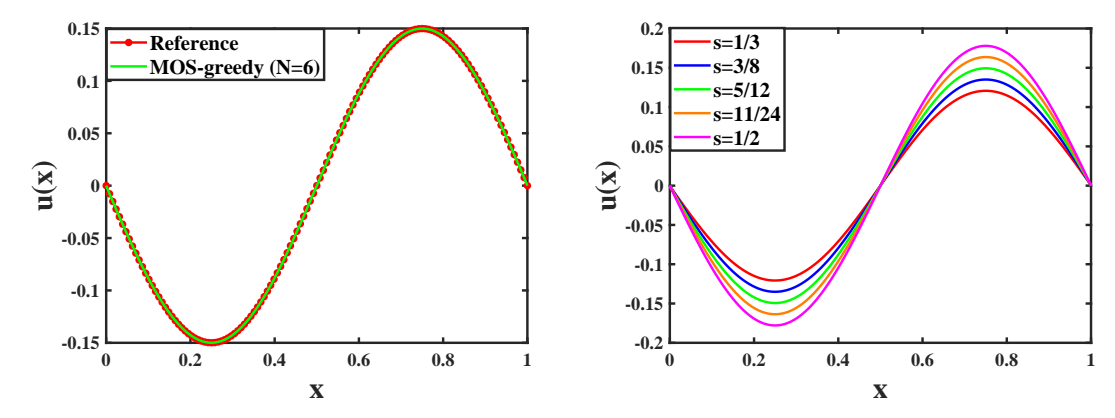


Figure 6: The mean of the reference and reduced order solution with N=6 (left) and reduced order solutions with different parameters (right).

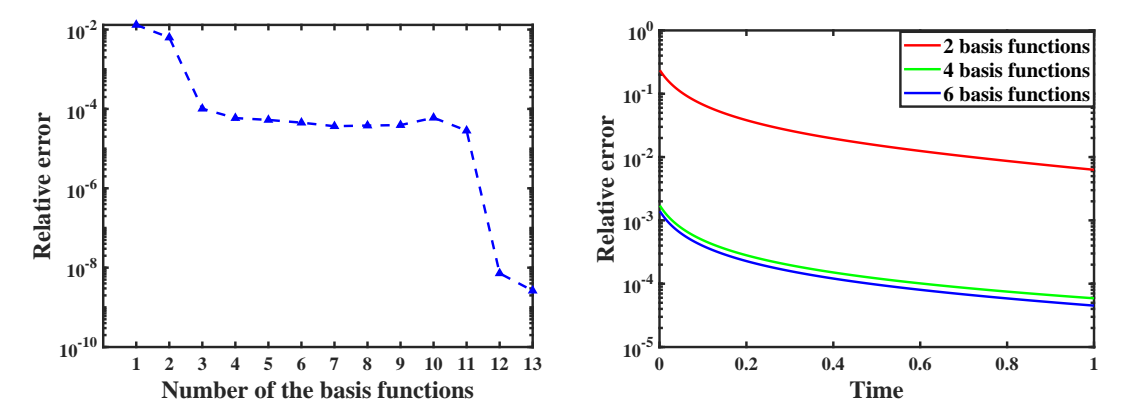


Figure 7: The average relative error corresponding to the different numbers of the basis functions (left) and the average relative error versus different time levels with N=2,4,6.

functions in Fig. 7 (left). The results demonstrate that the relative error decreases as the number of basis functions increases. While the rate of reduction slows slightly after 3 basis functions, the relative error continues to decline as the number of basis functions increases up to 11. To further demonstrate the relationship between relative error and time, we show the reduced order solutions with N = 2,4,6 in Fig. 7 (right). The relative error decreases against the time and the number of basis functions.

Finally, Fig. 8 compares the means and variances of the reference and reduced order solutions. The nearly identical profiles for both mean and variance confirm that the nonlinear ROMs provide an excellent approximation to the reference models, validating the effectiveness of the proposed method.

To highlight the advantages of the proposed methods, Table 1 lists the average online CPU time and average relative error of the FEM and MOS-greedy method

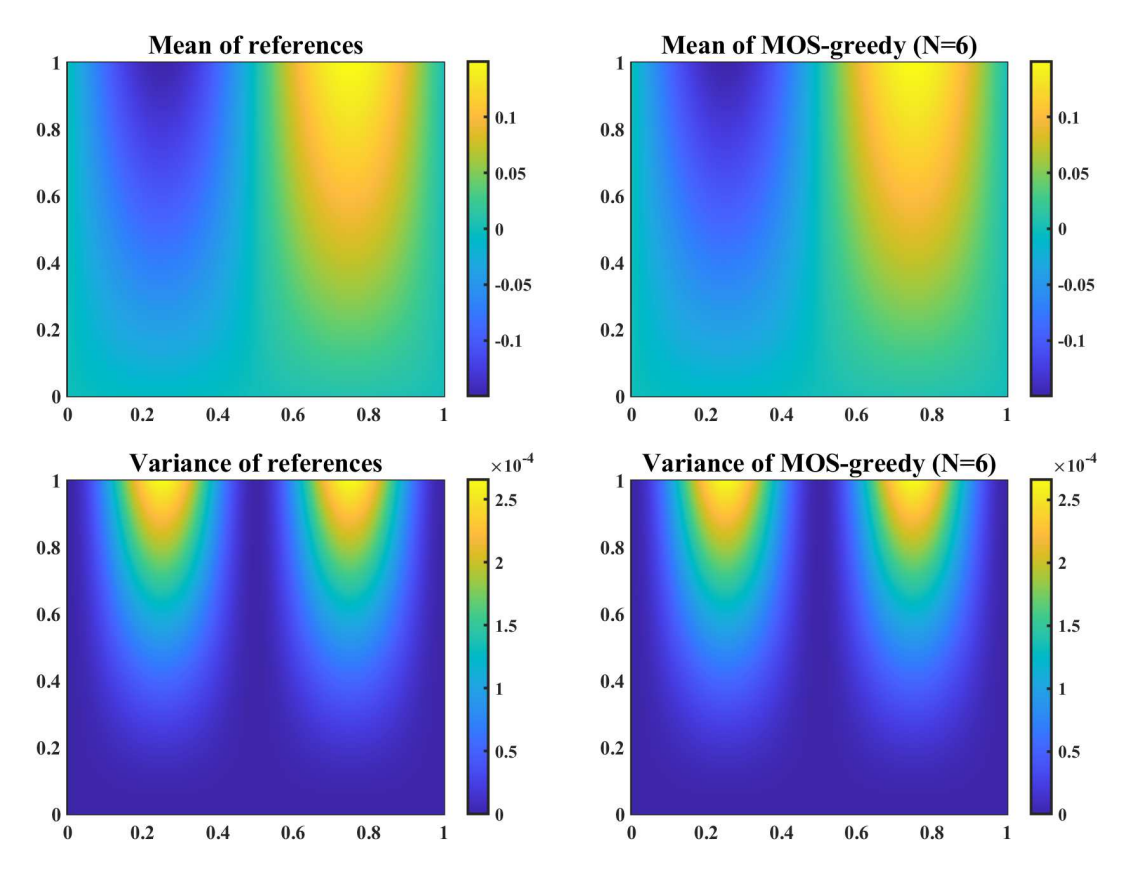


Figure 8: The mean and variance of the reference and reduced order solution with N=6. The first row is the mean profiles, and the second row is the variance profiles.

against the time. From the perspective of relative error, the proposed reduced model can provide good approximates of the full order model. Additionally, the MOS-greedy algorithm significantly improves computational efficiency. Compared to FEM, the proposed method performs well for both linear and nonlinear

Table 1: The average online CPU time and the average relative error by using FEM and MOS-greedy algorithm with $N\!=\!6$.

	Strategies	t=0.5	t=0.75	t=1
CPU time	FEM (Section 5.1)	1.261e+02s	1.461e+02s	1.521e+02s
	MOS-Greedy (Section 5.1)	2.081e-02s	4.381e-02s	5.561e-02s
	FEM (Section 5.2)	1.481e+02s	1.921e+02s	2.291e+02s
	MOS-Greedy(Section 5.2)	2.561e-02s	5.511e-02s	7.351e-02s
Relative error	MOS-Greedy (Section 5.1)	6.05e-04	6.00e-04	6.67e-04
	MOS-Greedy(Section 5.2)	9.67e-05	6.30e-05	4.51e-05

nonlocal models as time progresses, demonstrating its efficiency and effectiveness for solving nonlocal problems.

6 Conclusions

In this paper, we have proposed the method of snapshots and greedy (MOS-greedy) algorithm based on the frequency-domain for parameterized time-dependent nonlocal diffusion models. Since solving the full order model directly for each input parameter is expensive, we apply the Fourier transform and MOS-greedy algorithm to construct a ROM. The MOS-greedy algorithm is used to select the basis functions. For time-dependent nonlocal equations, the temporal term has a greater impact on the model reduction. The Fourier transform is employed to address this issue. It converts the time-dependent parabolic equation into a frequency-dependent elliptic equation. This can eliminate the influence of time and achieve the goal of model reduction, which improves computational efficiency. Then an offline-online computational decomposition is achieved in the MOS-greedy algorithm. This is very desirable for predicting the outputs of models for various stochastic influences.

In future work, we will continue to explore ROMs for nonlocal problems, such as the high-dimensional complex nonlocal equations, and compare the advantages and disadvantages of different methods for nonlocal equations.

Acknowledgments

The authors would like to thank the anonymous referees for their insightful comments on how to improve the quality of this paper.

The work of the first and the second authors is supported by the Guangdong Basic and Applied Basic Research Foundation, China (Grant 2024A1515012548). The work of the third author is supported by the National Natural Science Foundation of China (Grant 12401567), by the 2023 Guangzhou Basic and Applied Basic Research Project (Grant 2023A04J0035), and by the Talent Special Projects of School-level Scientific Research Programs under Guangdong Polytechnic Normal University (Grant 2022SDKYA025).

References

[1] E. Askari, F. Bobaru, R. B. Lehoucq, M. L. Parks, S. A. Silling, and O. Weckner, *Peridynamics for multiscale materials modeling*, J. Phys. Conf. Ser. 125 (2008), 12–78.

- [2] P. W. Bates, *On some nonlocal evolution equations arising in materials science*, in: Nonlinear Dynamics and Evolution Equations, Fields Inst. Commun. 48 (2006), 13–52.
- [3] P. Benner, S. Gugercin, and K. Willcox, *A survey of projection-based model reduction methods for parametric dynamical systems*, SIAM Rev. 57 (2015), 483–531.
- [4] H. Brezis and H. M. Nguyen, Nonlocal functionals related to the total variation and connections with image processing, Ann. PDE 4 (2016), 1–77.
- [5] O. Burkovska and M. Gunzburger, Regularity analyses and approximation of nonlocal variational equality and inequality problems, J. Math. Anal. Appl. 478 (2019), 1027–1048.
- [6] R. S. Cantrell and C. Cosner, Evolutionary stability of ideal free dispersal under spatial heterogeneity and time periodicity, Math. Biosci. 305 (2018), 71–76.
- [7] A. Cardone and G. Frasca-Caccia, *Numerical conservation laws of time fractional diffusion PDEs*, Fract. Calc. Appl. Anal. 25 (2022), 1459–1483.
- [8] S. Chakraborty and N. Zabaras, Efficient data-driven reduced-order models for high-dimensional multiscale dynamical systems, Comput. Phys. Comm. 230 (2018), 70–88.
- [9] S. Chaturantabut and D. C. Sorensen, *Nonlinear model reduction via discrete empirical interpolation*, SIAM J. Sci. Comput. 32 (2010), 2737–2764.
- [10] A. Ciomaga, D. Ghilli, and E. Topp, *Periodic homogenization for weakly elliptic Hamilton-Jacobi-Bellman equations with critical fractional diffusion*, Commun. Partial Diff. Equ. 47 (2022), 1–38.
- [11] C. Cosner, J. Davila, and S. Martinez, *Evolutionary stability of ideal free nonlocal dispersal*, J. Biol. Dyn. 6 (2012), 395–405.
- [12] N. N. Cuong, K. Veroy, and A. T. Patera, *Certified real-time solution of parametrized partial differential equations*, in: Handbook of Materials Modeling: Methods, Springer, (2005), 1529–1564.
- [13] M. D'Elia, Q. Du, M. Gunzburger, and R. Lehoucq, *Nonlocal convection-diffusion problems on bounded domains and finite-range jump processes*, Comput. Methods Appl. Math. 17 (2017), 707–722.
- [14] M. D'Elia and M. Gunzburger, *The fractional Laplacian operator on bounded domains as a special case of the nonlocal diffusion operator*, Comput. Math. Appl. 66 (2013), 1245–1260.
- [15] Q. Du, M. Gunzburger, R. B. Lehoucq, and K. Zhou, *Analysis and approximation of nonlocal diffusion problems with volume constraints*, SIAM Rev. 54 (2012), 667–696.
- [16] Q. Du, M. Gunzburger, R. B. Lehoucq, and K. Zhou, *A nonlocal vector calculus, non-local volume-constrained problems, and nonlocal balance laws*, Math. Models Methods Appl. Sci. 23 (2013), 493–540.
- [17] Q. Du, M. Gunzburger, R. B. Lehoucq, and K. Zhou, *Analysis of the volume-constrained peridynamic Navier equation of linear elasticity*, J. Elasticity 113 (2013), 193–217.
- [18] Q. Du, L. Ju, L. Tian, and K. Zhou, A posteriori error analysis of finite element method for linear nonlocal diffusion and peridynamic models, Math. Comp. 82 (2013), 1889–1922.
- [19] Q. Du, Y. Tao, X. Tian, and J. Yang, Robust a posteriori stress analysis for quadrature

- collocation approximations of nonlocal models via nonlocal gradients, Comput. Methods Appl. Mech. Engrg. 310 (2016), 605–627.
- [20] Q. Du and X. Tian, *Robust discretization of nonlocal models related to peridynamics*, in: Meshfree Methods for Partial Differential Equations VII. Lecture Notes in Computational Science and Engineering, Springer, Cham 100 (2015), 97–113.
- [21] Q. Du, J. Yang, and Z. Zhou, *Analysis of a nonlocal-in-time parabolic equation*, Discrete Contin. Dyn. Syst. Ser. A 22 (2017), 339–368.
- [22] Q. Du and K. Zhou, *Mathematical analysis for the peridynamic nonlocal continuum the-ory*, ESAIM Math. Model. Numer. Anal. 45 (2011), 217–234.
- [23] P. Fife, *Some nonclassical trends in parabolic and parabolic-like evolutions*, in: Trends in Nonlinear Analysis, Springer (2003), 153–191.
- [24] J. P. Fink and W. C. Rheinboldt, *On the error behavior of the reduced basis technique for nonlinear finite element approximations*, Z. Angew. Math. Mech. 63 (1983), 21–28.
- [25] J. P. Fink and W. C. Rheinboldt, Solution manifolds and submanifolds of parametrized equations and their discretization errors, Numer. Math. 45 (1984), 323–343.
- [26] G. Gilboa and S. Osher, *Nonlocal operators with applications to image processing*, Multiscale Model. Simul. 7 (2008), 1005–1028.
- [27] A. Goffi, Transport equations with nonlocal diffusion and applications to Hamilton-Jacobi equations, J. Evol. Equ. 21 (2021), 4261–4317.
- [28] Q. Guan, M. D. Gunzburger, C. Webster, and G. Zhang, *Reduced basis methods for nonlocal diffusion problems with random input data*, Comput. Methods Appl. Mech. Engrg. 317 (2017), 746–770.
- [29] M. Gunzburger and O. Burkovska, *Affine approximation of parametrized kernels and model order reduction for nonlocal and fractional Laplace models*, SIAM J. Numer. Anal. 58 (2019), 1469–1494.
- [30] M. Gunzburger and R. B. Lehoucq, *A nonlocal vector calculus with application to non-local boundary value problems*, Multiscale Model. Simul. 8 (2010), 1581–1598.
- [31] C. O. Lee, J. Lee, and D. Sheen, *A frequency-domain parallel method for the numerical approximation of parabolic problems*, Comput. Methods Appl. Mech. Engrg. 169 (1999), 19–29.
- [32] T. Mengesha and Q. Du, Characterization of function spaces of vector fields and an application in nonlinear peridynamics, Nonlinear Anal. 140 (2016), 82–111.
- [33] N. C. Nguyen, G. Rozza, and A. T. Patera, *Reduced basis approximation and a posteriori* error estimation for the time-dependent viscous Burgers' equation, Calcolo 46 (2009), 157–185.
- [34] A. M. Quarteroni, A. Manzoni, and F. Negri, *Construction of RB spaces by SVD-POD*, in: Reduced Basis Methods for Partial Differential Equations, Springer (2015), 123–126.
- [35] A. M. Quarteroni, G. Rozza, and A. Manzoni, *Certified reduced basis approximation for parametrized partial differential equations and applications*, J. Math. Ind. 1 (2011), 1–49.

- [36] G. Rozza, D. B. P. Huynh, and A. T. Patera, *Reduced basis approximation and a posteriori error estimation for affinely parametrized elliptic coercive partial differential equations*, Arch. Comput. Methods Eng. 15 (2008), 229–275.
- [37] A. Sartori, A. Cammi, L. Luzzi, and G. Rozza, *Reduced basis approaches in time-de*pendent non-coercive settings for modelling the movement of nuclear reactor control rods, Commun. Comput. Phys. 20 (2016), 23–59.
- [38] R. L. Schilling, *Financial modelling with jump processes*, J. Roy. Statist. Soc. Ser. A 168 (2004), 250–251.
- [39] S. K. Star, G. Stabile, F. Belloni, G. Rozza, and J. Degroote, *A novel iterative penalty method to enforce boundary conditions in finite volume POD-Galerkin reduced order models for fluid dynamics problems*, Commun. Comput. Phys. 30 (2021), 34–66.
- [40] X. Tian and Q. Du, Analysis and comparison of different approximations to nonlocal diffusion and linear peridynamic equations, SIAM J. Numer. Anal. 51 (2013), 3458–3482.
- [41] X. Tian and Q. Du, *A class of high order nonlocal operators*, Arch. Ration. Mech. Anal. 222 (2016), 1521–1553.
- [42] X. Tian and Q. Du, *Trace theorems for some nonlocal function spaces with heterogeneous localization*, SIAM J. Numer. Anal. 49 (2017), 1621–1644.
- [43] X. Tian, Q. Du, and M. Gunzburger, Asymptotically compatible schemes for the approximation of fractional Laplacian and related nonlocal diffusion problems on bounded domains, Adv. Comput. Math. 42 (2016), 1363–1380.
- [44] K. Veroy, C. Prud'homme, D. Rovas, and A. T. Patera, *A posteriori error bounds for reduced-basis approximation of parametrized noncoercive and nonlinear elliptic partial differential equations*, in: Proceedings of 16th AIAA Computational Fluid Dynamics Conference, (2003), 2003–3847.
- [45] G. Wang and Q. Liao, Reduced basis stochastic Galerkin methods for partial differential equations with random inputs, Appl. Math. Comput. 463 (2024), 128375.
- [46] Z. Wang, B. Mcbee, and T. Iliescu, *Approximate partitioned method of snapshots for POD*, J. Comput. Appl. Math. 307 (2016), 374–384.
- [47] D. R. Witman, M. Gunzburger, and J. Peterson, *Reduced-order modeling for nonlocal diffusion problems*, Internat. J. Numer. Methods Fluids 83 (2017), 307–327.